The Lateral and the Angular Structure Functions of Electron Showers

Koichi KAMATA and Jun NISHIMURA*

Scientific Research Institute, Itabashi, Tokyo
*Institute for Nuclear Study, University of Tokyo, Tokyo

Abstract

Lateral and angular distribution functions of the electron showers are derived analytically with and without the Landau approximation including ionization loss. Tables and the numerical results of these functions are presented, and their results are applied to the analysis of high energy cosmic ray phenomena.

Relations between the present theories and the others are discussed critically, and it is shown that the other theories can be regarded as special cases of our theories.

§1. Introduction

Many ingenious works on the theory of electron-photon cascades have hitherto been developed, by which the fundamental behavior of cascade showers have been made clear to a great extent in last two decades. In the earlier stage of the shower study, rather indirect proofs on the applicability of the theory were furnished by comparison of one dimensional cascade

theory with experiments of the cosmic rays.

However the recent improvements of the experimental techniques and the accumulation of the data have required the three-dimensional treatment of the theory of the cascade showers. The accurate knowledge of the lateral distribution of cascade showers becomes indispensable in the analysis of extensive air showers and other cosmic-ray phenomena at high energies. Several works have been made along this line,[1,2] but their applicabilities to practical purposes seem to be limited.

Molière's lateral structure function[3] is the one which has been extensively used for comparison with experiment, but the approximations made in his theory seem to be inadequate for practical application. The function was derived numerically as a solution of the Landau equation in the approximation A.[4] For the contribution of the low energy particles, he used Arley's approximation, which is known to be inaccurate in the low energy side. In addition to this, his function is limited to the region of shower maximum, and it is more or less inconvenient for practical application.

In the theory of Roberg and Nordheim,[5] the low energy particles were treated accurately, but only the second moments of the structure functions were obtained instead of the functions themselves.

Eyges and Fernbach,[1] and Chartres and Messel[2] obtained the stracture function in a more accurate way, but, as will be shown later, the applicability of their theories is still limited.

In our previous papers,[6] a mathematical method was developed to get the solution of the Landau equation including ionization loss. Then, the lateral and the angular structure functions of a cascade shower at any depth were obtained analytically in the approximation B.[4] In this paper a further development of our theory is presented, and the theory is further extended to get the solution without using the Landau approximation.

The lateral distribution of "the energy flow" of shower particles is also useful for the analysis of extensive air showers. It is the lateral distribution of the energy density contained in shower particles. The analytical solutions are derived, and the numerical calculation is carried out at shower maximum.

Application of our theory is made to the analysis of the extensive air showers and the electron showers observed in photographic emulsions.

For the analysis of the extensive air showers, the effect of the variation of the air density on the lateral structure function is calculated, and the second moment of the lateral structure function thus derived in the isothermal atmosphere is compared with the one in homogeneous matter.

The distribution of shower particles near the shower axis is closely related to the core structure of extensive air showers. Thus the character-

istic features of the structure function at small distance from the axis are carefully examined in Appendix I.

§2.   Approximations and Assumptions made in Our Calculations

The electrons in a cascade shower suffer the deflection by the Coulomb scattering in traversing the matter.   Hence the shower spreads side-wise when it develops through the matter.   The spreads due to the deflections in the radiation and pair creation processes are known to be negligible compared with the contribution of the Coulomb scattering except at the biginning of the shower development.   Thus the three dimensional cascade theory can be constructed from the one dimensional cascade theory and the theory of multiple Coulomb scattering of a particle.   For the one dimensional cascade theory, we refer to Approximation B in reference 4.

The details of the approximation B are as follows.

In this approximation it is assumed that electrons lose their energy only through radiation and ionization processes, and photons by pair creation process.   Other electromagnetic interactions such as Compton scattering and trident formation by electrons are neglected.

For the probability of radiation and pair creation processes the Bethe-Heitler cross sections for the complete screening are adopted.   Ionization loss of an electron is assumed to be independent of the energy of the electron, and is equal to ε per radiation unit.

These assumptions are approximately justified without introducing a serious error for high energy particles and for media of low atomic numbers.   Since the limitation of this approximation has been repeatedly explained in many papers,[4][7] we will not reproduce it here.

The probability for an electron of energy E traversing one radiation length of matter to emit a photon of energy between Ev and $E(v+dv)$ is given in the case of the complete screening by

$$\varphi(v)\,dv = \left[1 + (1-v)^2 - (1-v)\left(\frac{2}{3} - 2b\right)\right]dv/v, \qquad (2\cdot1)$$

where $b = 1/[18\ln(183\,Z^{-1/3})]$ and Z is the atomic number of traversing material.

The probability, $\psi(u)\,du$, for a photon of energy W traversing one radiation length to produce an electron pair, in which the positron has the energy between Wu and $W(u+du)$ is given in the case of the complete screening by

$$\psi(u)\,du = \left[u^2 + (1-u)^2 - \left(\frac{2}{3} - 2b\right)u(1-u)\right]du. \qquad (2\cdot2)$$

The total probability for pair creation per radiation length is defined by

$$\sigma(W) = \int_{m_e/W}^{1-m_e/W} \psi(u)\,du, \tag{2\cdot3}$$

and, from the formula (2·2), is given by

$$\sigma(W) = \sigma_0 = (7/9) - (b/3). \tag{2\cdot4}$$

It should be noticed here that, the above cross sections have the fractional forms which does not depend explicitly on the energy of the particle, but only on the ratio of the energy of the incident particle to that of the secondary particle. We can thus apply the Mellin transformation to get the solution of the cascade equation.

Recently the limit of applicability of the complete screening cross sections at very high energies has been critically discussed by Landau and Pomeranchuk.[8] They pointed out that, at very high energy, the path length of an electron which is effective in the collision process becomes so long that the interference effects of the adjacent atoms should be taken into account, and that the cross section should decrease in the high energy region.

Even if the cross section should fall off at very high energies, the average energy of shower particles would soon decrease by orders of magnitude by the rapid multiplication of particles. Thus these effects, if exists any, should concern only the beginning stages of shower development and the overall behavior should suffer little change.

Let $\pi(E, r, \theta, t)dEdrd\theta$ be the average number of electrons with energy between E and $E+dE$ travelling at an angle $(\theta, d\theta)$ with the shower axis at the position (r, dr) at the depth t, and $\gamma(W, r, \theta, t)\,dWdrd\theta$ the corresponding quantity for photons with energy between W and $W+dW$.

In the electron-photon cascade, the number of electrons with energy (E, dE) changes in a given thickness dt by the following effects;

(a) The photons with energy (W, dW) at the depth t produce the electrons of energy (E, dE) in a thickness dt. The number of these electrons is given by

$$dEdt\, 2\int_E^\infty \gamma(W, t)\psi(E/W)dW/W = dEdt\, 2\int_0^1 \gamma(E/u, t)\psi(u)du/u, \tag{2\cdot5}$$

where $\psi(u)du$ is the differential pair creation probability given by (2·2).

The equation (2·5) is written in an operational form as

$$B'\gamma. \tag{2\cdot5a}$$

(b) The electrons in the energy interval (E, dE) escape this interval by the radiation loss, and the electrons with energy E' larger than E fall

into this interval also by the radiation loss. The net change is

$$dEdt \left[-\int_0^E \pi(E, t)\varphi(W/E)dW/E + \int_E^\infty \pi(E', t)\varphi(E'-E/E')dE'/E \right]$$

$$= dEdt \int_0^1 \left[-\pi(E, t) + \frac{1}{1-v}\pi(E/1-v, t) \right] \varphi(v)dv, \qquad (2\cdot6)$$

where $\varphi(v)dv$ is the radiation probability given by $(2\cdot1)$. The equation is also written in an operational form as

$$-A'\pi. \qquad (2\cdot6a)$$

(c) An electron loses an amount $\varepsilon\, dt$ of energy in a thickness dt by the ionization process. Then $\pi(E+dE)\,\varepsilon\, dt$ electrons enter the interval (E, dE) and $\pi(E)\,\varepsilon\, dt$ electrons escape this interval. The net variation in the number of electrons by ionization loss is

$$\left\{ \pi(E+dE) - \pi(E) \right\} \varepsilon\, dt = \varepsilon \frac{\partial\pi}{\partial E}dEdt. \qquad (2\cdot7)$$

Consequently, the variation in the number of electrons can be expressed by

$$\frac{\partial\pi}{\partial t} = 2\int_0^1 \gamma(E/u, t)\psi(u)du/u$$

$$+ \int_0^1 \left[\frac{1}{1-v}\pi(E/1-v, t) - \pi(E, t) \right]\varphi(v)dv + \varepsilon\frac{\partial\pi}{\partial E}. \qquad (2\cdot8)$$

Correspondingly, the variation in the number of photons can be expressed by

$$\frac{\partial\gamma}{\partial t} = \int_0^1 \pi(W/u, t)\varphi(v)dv/v - \sigma_0\gamma(W, t), \qquad (2\cdot9)$$

where σ_0 is the total cross section of pair creation given by $(2\cdot4)$.

Then, the diffusion equations for the one-dimensional cascade showers are given in an operational form as

$$\frac{\partial\pi}{\partial t} = -A'\pi + B'\gamma + \varepsilon\frac{\partial\pi}{\partial E}, \qquad (2\cdot8a)$$

$$\frac{\partial\gamma}{\partial t} = C'\pi - \sigma_0\gamma. \qquad (2\cdot9a)$$

Let us next consider the lateral and angular variation of electrons by the Coulomb scattering in traversing a thickness dt.

Let $\sigma(\theta)d\theta$ be the probability that an electron is scattered through an angle $(\theta, d\theta)$ while travelling a given thickness. The variation in the

number of electrons in the spatial and angular intervals (r, dr) and $(\theta, d\theta)$ is obtained as follows.

(a)   An electron at a position (r, dr) travelling in the direction θ with the shower axis suffers the lateral displacement θdt in thickness dt. Then, an electron at r at the depth t will be at $r + \theta dt$ at the depth $t + dt$. Hence

$$\pi(t + dt, r, \theta) = \pi(t, r - \theta dt, \theta)$$

$$= \pi(t, r, \theta) - \theta dt \frac{\partial \pi}{\partial r} . \qquad (2 \cdot 10)$$

(b)   An electron travelling in the direction $(\theta', d\theta')$ at the depth t will be scattered into $(\theta, d\theta)$ by the Coulomb scattering. Then the variation in the number of electrons within an interval $(\theta, d\theta)$ caused by the scattering while travelling the thickness dt is given by

$$dt \left[\int_{-\infty}^{+\infty} \sigma(\theta - \theta') \pi(\theta') d\theta' - \int_{-\infty}^{+\infty} \sigma(\theta') d\theta' \pi(\theta) \right], \qquad (2 \cdot 11)$$

or, in an operational form, by

$$\sigma' \pi .$$

Thus the basic diffusion equations for the three dimensional cascade theory are:

$$\frac{\partial \pi}{\partial t} + \theta \frac{\partial \pi}{\partial r} = -A' \pi + B' \gamma + \sigma' \pi - \varepsilon \frac{\partial \pi}{\partial E}, \qquad (2 \cdot 12)$$

$$\frac{\partial \gamma}{\partial t} + \theta \frac{\partial \gamma}{\partial r} = C' \pi - \sigma_0 \gamma . \qquad (2 \cdot 13)$$

The probability for an electron of being scattered by the Coulomb field of a nucleous, assuming the point charge distribution, is approximately represented by[4]

$$\sigma(\theta) d\theta = \frac{1}{4\pi \ln(181 Z^{-1/3})} \left(\frac{E_s}{E} \right)^2 \frac{d\theta}{\theta^4}, \qquad (2 \cdot 14)$$

where $E_s = 2\pi (137)^{1/2} m_e c^2 = 21 \text{MeV} .$

The finite size of the nucleous and the screening of the Coulomb field by the outer electrons, will make the probability smaller than that given by the formula $(2 \cdot 14)$ for large and small θ respectively. Thus, Williams[9] approximated the probability as follows:

$$\sigma(\theta) d\theta = 0 \qquad\qquad\qquad \theta < \theta_{\min},$$

$$\sigma(\boldsymbol{\theta})d\boldsymbol{\theta} = \text{the formula } (2\cdot14) \quad \theta_{\min} < \theta < \theta_{\max},$$

and $\qquad \sigma(\boldsymbol{\theta})d\boldsymbol{\theta} = 0 \qquad\qquad \theta > \theta_{\max},$

where $\qquad\qquad \theta_{\min} = \lambda / a,$

$$\theta_{\max} = \lambda / d,$$

and $2\pi\lambda$ is the de Broglie wave length of an incident electron, d the radius of the charge distribution of the nucleus, and "a" the Bohr radius of the atom.

Comparison of this expression with the experimental data was made by Stanford group.[10] Although this approximation is only a crude one, we take this expression to start with in the treatment of the spread of an electron shower.

Following Williams, $\pi(t, \boldsymbol{\theta}' + \boldsymbol{\theta})$ is expanded in the Taylor series of $\boldsymbol{\theta}'$, and the formula $(2\cdot11)$ then becomes

$$dt\left[\int_{-\infty}^{\infty}\left\{\pi(\boldsymbol{\theta}) + \boldsymbol{\theta}'\nabla_{\theta}\,\pi(\boldsymbol{\theta}) + \frac{(\boldsymbol{\theta}')^2}{2!}\nabla_{\theta}^2\pi(\boldsymbol{\theta}) + \cdots\right\}\sigma(\boldsymbol{\theta}')d\boldsymbol{\theta}' \right.$$
$$\left. - \int_{-\infty}^{\infty}\pi(\boldsymbol{\theta})\sigma(\boldsymbol{\theta}')d\boldsymbol{\theta}'\right]. \qquad (2\cdot15)$$

Because of the axial symmetry of the scattering probability, the second term in the series in $(2\cdot15)$ vanishes. The third term is equal to the mean square angle of the scattering, i.e.,

$$\int_{-\infty}^{\infty}(\boldsymbol{\theta}')^2\sigma(\boldsymbol{\theta}')d\boldsymbol{\theta}' = 2\int_{\theta_{\min}}^{\theta_{\max}}(\boldsymbol{\theta}')^2\sigma(\boldsymbol{\theta}')2\pi\boldsymbol{\theta}'d\boldsymbol{\theta}'$$
$$= \frac{(E_s/E)^2}{\ln(181Z^{-1/3})}\ln\frac{\theta_{\max}}{\theta_{\min}}, \qquad (2\cdot16)$$

where $\qquad E_s = 21$ Mev.

Taking $\ln\dfrac{\theta_{\max}}{\theta_{\min}} = \ln(181Z^{-1/3})$, as given by Williams, the formula $(2\cdot16)$ becomes $\dfrac{1}{2}(E_s/E)^2$.

Then the equations $(2\cdot12)$ and $(2\cdot13)$ become

$$\left(\frac{\partial}{\partial t} + \boldsymbol{\theta}\frac{\partial}{\partial r}\right)\pi = -A'\pi + B'\pi + \sigma'\gamma + \frac{E_s^2}{4E^2}\nabla_{\theta}^2\pi + \varepsilon\frac{\partial\pi}{\partial E}, \qquad (2\cdot17)$$

$$\left(\frac{\partial}{\partial t} + \boldsymbol{\theta}\frac{\partial}{\partial r}\right)\gamma = C'\pi - \sigma_0\gamma. \qquad (2\cdot18)$$

These are referred to as the Landau equations. Those without the above expansion for the scattering are referred to as the equations "without

Landau approximation", the detailed description of which will be given in a later section.

§3. Structure Functions under the Landau Approximation

A) Mathematical treatment

In our previous paper,[6] a mathematical method to get the analytical solution for the angular structure function of shower particles was presented. Similar treatment is also possible for the lateral structure function, although it was not presented there. Thus, it seems desirable to give the details of this method in this section.

As shown in the previous section, the Landau equations including ionization loss is given by

$$\left(\frac{\partial}{\partial t}+\theta\frac{\partial}{\partial r}\right)\pi = -A'\pi + B'\gamma + \frac{E_s{}^2}{4E^2}\left(\frac{\partial^2}{\partial\theta_1^2}+\frac{\partial^2}{\partial\theta_2^2}\right)\pi + \varepsilon\frac{\partial\pi}{\partial E}, \qquad (3\cdot1)$$

$$\left(\frac{\partial}{\partial t}+\theta\frac{\partial}{\partial r}\right)\gamma = C'\pi - \sigma_0\gamma. \qquad (3\cdot2)$$

In order to get the solution of these equations, functional transformations are used as in many problems of the similar type. Multiplying the both side of the equations $(3\cdot1)$ and $(3\cdot2)$ by $\exp(i(rx)+i(\theta\varsigma))$ and integrating with respect to r and θ, we get

$$\left(\frac{\partial}{\partial t}-x\frac{\partial}{\partial\varsigma}\right)f = -A'f + B'g - \frac{E_s{}^2\zeta^2}{4E^2}f + \varepsilon\frac{\partial}{\partial E}f, \qquad (3\cdot1a)$$

$$\left(\frac{\partial}{\partial t}-x\frac{\partial}{\partial\varsigma}\right)g = C'f - \sigma_0 g, \qquad (3\cdot2a)$$

where f and g are the Fourier transforms of π and γ, which are defined by

$$f(x,\varsigma)=\frac{1}{4\pi^2}\int\int\int_{-\infty}^{+\infty}\int \pi(r,\theta)e^{i(rx)+i(\theta\varsigma)}drd\theta, \qquad (3\cdot3)$$

$$g(x,\varsigma)=\frac{1}{4\pi^2}\int\int\int_{-\infty}^{+\infty}\int \gamma(r,\theta)e^{i(rx)+i(\theta\varsigma)}drd\theta, \qquad (3\cdot4)$$

and the vectors x and ς have the components (x_1, x_2) and (ζ_1, ζ_2) respectively.

Eliminating g from the above equations we get

$$\left\{\left(\frac{\partial}{\partial t}-x\frac{\partial}{\partial\varsigma}\right)^2 + (A'+\sigma_0)\left(\frac{\partial}{\partial t}-x\frac{\partial}{\partial\varsigma}\right) + (A'\sigma_0 - B'C')\right\}f(x,\varsigma) =$$

$$=\left(\frac{\partial}{\partial t}-x\frac{\partial}{\partial\varsigma}+\sigma_0\right)\left(-\frac{E_s^2\varsigma^2}{4E^2}+\varepsilon\frac{\partial}{\partial E}\right)f(x,\varsigma). \tag{3.5}$$

Since the lateral structure function of electrons $\pi_2(E_0,E,r,t)\ 2\pi r dr$ is given by $\pi_2=\int\int_{-\infty}^{+\infty}\pi(E_0,E,r,\theta,t)\ 2\pi\theta d\theta$, it follows directly from the formula (3.3) and (3.4) that

$$\pi_2(E_0,E,r,t)=\int\int_{-\infty}^{+\infty}e^{-i(xr)}f(x,0)dx=\int_0^{\infty}f(x,0)J_0(xr)2\pi xdx, \tag{3.6}$$

where J_0 is the Bessel function, and $x=(x_1^2+x_2^2)^{\frac{1}{2}}$ and $r=(y_1^2+y_2^2)^{\frac{1}{2}}$.

Similarly the angular structure function is given by

$$\pi_1(E_0,E,\theta,t)=\int_0^{\infty}f(0,\zeta)J_0(\zeta\theta)2\pi\zeta d\zeta. \tag{3.7}$$

Thus we have only to get the solution of $f(x,0)$ from equation (3.5) in order to obtain the lateral structure function. We can not, however, put $\varsigma=0$ immediately in equation (3.5), because in this equation there exist the derivatives with respect to ς. Taking the direction of the vector ς to be parallel to x, the equation for the function $f(x,\zeta_1,\zeta_2=0)$ is given by

$$\left\{\left(\frac{\partial}{\partial t}-x\frac{\partial}{\partial\zeta_1}\right)^2+(A'+\sigma_0)\left(\frac{\partial}{\partial t}-x\frac{\partial}{\partial\zeta_1}\right)+(A'\sigma_0-B'C')\right\}f(\zeta_2=0)$$

$$=\left(\frac{\partial}{\partial t}-x\frac{\partial}{\partial\zeta_1}+\sigma_0\right)\left(-\frac{E_s^2\zeta_1^2}{4E^2}+\varepsilon\frac{\partial}{\partial E}\right)f(\zeta_2=0). \tag{3.8}$$

Here we introduce the variables ξ and t' defined by

$$t=t'$$

and

$$\zeta_1=x(\xi-t').$$

Then, we have

$$\frac{\partial}{\partial t'}=\frac{\partial}{\partial t}-x\frac{\partial}{\partial\zeta_1}.$$

The equation (3.8) now becomes

$$\left\{\frac{\partial^2}{\partial t'^2}+(A'+\sigma_0)\frac{\partial}{\partial t'}+(A'\sigma_0-B'C')\right\}f$$

$$=\left(\frac{\partial}{\partial t'}+\sigma_0\right)\left[-\frac{E_s^2x^2}{4E^2}(\xi-t')^2+\varepsilon\frac{\partial}{\partial E}\right]f. \tag{3.9}$$

As shown by Landau Rumer,[11] one-dimensional cascade function under the boundary condition corresponding to a single incident electron of

energy E_0 is given by

$$\pi = \frac{1}{2\pi i} \int ds \left(\frac{E_0}{E}\right)^s \frac{1}{E} \left(H_1(s)e^{\lambda_1(s)t} + H_2(s)e^{\lambda_2(s)t}\right),$$

where all notations are the same as those in reference 4, and s is a complex variable and the path of integration runs parallel to the imaginary axis.

This is just the solution of equation[*]

$$\left\{\frac{\partial^2}{\partial t^2} + (A' + \sigma_0)\frac{\partial}{\partial t} + (A'\sigma_0 - B'C')\right\}f = 0,$$

which is given by putting E_s and ε zero in the equation (3·9). Thus, we get the solution of the equation (3·9) in a successive manner, i.e. in a power series of $\dfrac{E_s^2 x^2}{4E^2}$ and (ε/E), and it is given by

$$f_2 = \frac{1}{4\pi^2 i} \int_{\delta-i\infty}^{\delta+i\infty} \left(\frac{E_0}{E}\right)^s \frac{ds}{E} \left\{\sum_{m=n}^{\infty}\sum_{n=0}^{\infty} \left(\frac{-E_s^2 x^2}{4E^2}\right)^m \left(\frac{-\varepsilon}{E}\right)^n \phi_{m,n}(s,t)\right\}, \quad (3\cdot10)$$

where $\phi_{m,n}$ is given by the equation

$$\left[\frac{\partial^2}{\partial t^2} + (A_{(s+2m+n)} + \sigma_0)\frac{\partial}{\partial t} + (A\sigma_0 - BC)_{s+2m+n}\right]\Phi_{m,n}$$

$$= \left(\frac{\partial}{\partial t} + \sigma_0\right)\left\{(\xi - t)^2\Phi_{m-1,n} + (s+2m+n)\Phi_{m,n-1}\right\} \quad (3\cdot11)$$

with $\phi_{m,n} = \lim_{(\xi-t)\to 0} \Phi_{m,n}$,

A, B and C are defined by

$$A'E^{-(s+2m+n+1)} = E^{-(s+2m+n+1)}A(s+2m+n),$$

$$B'E^{-(s+2m+n+1)} = E^{-(s+2m+n+1)}B(s+2m+n),$$

$$C'E^{-(s+2m+n+1)} = E^{-(s+2m+n+1)}C(s+2m+n),$$

and $A(s) = \left(\frac{4}{3} + 0.027\right)\left(\frac{d}{ds}\ln\Gamma(s+1) + 0.5772 - 1 + \frac{1}{s+1}\right)$

$$+ \frac{1}{2} - \frac{1}{(s+1)(s+2)}, \quad (3\cdot12)$$

$$B(s) = 2\left(\frac{1}{s+1} - \frac{1.360}{(s+2)(s+3)}\right), \quad (3\cdot13)$$

$$C(s) = \frac{1}{s+2} + \frac{1.360}{s(s+1)}, \quad (3\cdot14)$$

$$\sigma_0 = 0.7733. \quad (3\cdot15)$$

---

[*] Hereafter we write t instead of t' for brevity.

The numerical values of $A(s)$, $B(s)$ and $C(s)$ are given in reference 4. $\varPhi_{0,0}$ satisfies the following equation

$$\left[\frac{\partial^2}{\partial t^2}+\left\{A(s)+\sigma_0\right\}\frac{\partial}{\partial t}+A(s)\sigma_0-B(s)C(s)\right]\varPhi_{0,0}=0 .$$

Then it follows that

$$\varPhi_{0,0}=H_1(s)e^{\lambda_1(s)t}+H_2(s)e^{\lambda_2(s)t} , \tag{3·16}$$

$$H_1(s)=\frac{\sigma_0+\lambda_1(s)}{\lambda_1(s)-\lambda_2(s)}, \quad H_2(s)=-\frac{\sigma_0+\lambda_2(s)}{\lambda_1(s)-\lambda_2(s)} , \tag{3·17}$$

$$\lambda_1(s)=\frac{1}{2}\left[-\left(A(s)+\sigma_0\right)+\left\{\left(A(s)-\sigma_0\right)^2+4B(s)C(s)\right\}^{\frac{1}{2}}\right], \tag{3·18}$$

and

$$\lambda_2(s)=\frac{1}{2}\left[-\left(A(s)+\sigma_0\right)-\left\{\left(A(s)-\sigma_0\right)^2+4B(s)C(s)\right\}^{\frac{1}{2}}\right]. \tag{3·19}$$

Further (3·16) satisfies the boundary conditions

$$\varPhi_{0,0}(s, 0)=1, \quad \left.\frac{\partial\varPhi_{0,0}(s, t)}{\partial t}\right|_{t=0}=-A(s) , \tag{3·20}$$

corresponding to the shower initiated by a single electron of energy E_0.

The solution of equation (3·11) is now given by the recurrence formula:

$$\varPhi_{m, n}(s, \xi-t, t)=\int_0^t \varPhi_{0,0}(s+2m+n, t-t')\left\{(\xi-t')^2\varPhi_{m-1, n}(s, \xi-t', t')\right.$$

$$\left.+(s+2m+n)\varPhi_{m, n-1}(s, \xi-t', t')\right\} dt' . \tag{3·21}$$

This can be proved simply by substituting (3·21) in (3·11). From the formulae (3·20) and (3·21), we find

$$\phi_{m, n}\lesssim|\phi_{0,0}(s, t)|\frac{2^n\Gamma(s+m+n+1)t^{3m+n}}{3^m\Gamma(s+1)\Gamma(m+1)\Gamma(n+1)}$$

$$\lesssim|\phi_{0,0}(s, t)|2^s(4/3)^m 8^n t^{3m+n} \tag{3·22}$$

for any values of s and t, in which $|\phi_{0,0}(s, t)|$ is the largest value of $\phi_{0,0}(s, t')$ in the region where t' varies between 0 and t.

Then it follows that the double series in (3·10) is uniformly and absolutely convergent if $E>\dfrac{E_s x t^{\frac{3}{2}}}{3}$ and $E>8\varepsilon t$, and the above argument is merely a general extension of the one given by Bhabha-Chackrabarty.[12]

Now, as was shown in our previous paper, we introduce the Mellin transforms, $\mathfrak{M}_2$ (p, q, s, t), of the function $F(\alpha, \beta, s, t)$ and put

$$\mathfrak{M}_2(m, n, s, t) = \frac{\phi_{m,n}(s, t)}{\Gamma(m+1)\Gamma(n+1)} \ . \tag{3.23}$$

Then the double series in (3·10) can be written as

$$\sum_{m=0}^{\infty} \sum_{n=0}^{\infty} \left(-\frac{E_s^2 x^2}{4E^2}\right)^m \left(-\frac{\varepsilon}{E}\right)^n \phi_{m,n}(s, t)$$

$$= \int\int_0^{\infty} e^{-\alpha\frac{E_s^2 x^2}{4E^2} - \beta\frac{\varepsilon}{E}} F(\alpha, \beta, s, t) d\alpha d\beta \ . \tag{3.24}$$

Moreover, it follows by the inverse Mellin transformation that the formula (3·24) becomes

$$\sum_{m=0}^{\infty} \sum_{n=0}^{\infty} \left(-\frac{E_s^2 x^2}{4E^2}\right)^m \left(-\frac{\varepsilon}{E}\right)^n \phi_{m,n}(s, t)$$

$$= -\frac{1}{4\pi^2} \int\int_0^{\infty} d\alpha d\beta e^{-\frac{\alpha E_s^2 x^2}{4E^2} - \beta\frac{\varepsilon}{E}} \int\int_{-i\infty}^{i\infty} dp dq \frac{\mathfrak{M}_2(p, q, s, t)}{\alpha^{p+1}\beta^{q+1}}. \tag{3.25}$$

Since the double series is uniformly and absolutely convergent for $E > \frac{E_s x t^{\frac{3}{2}}}{3}$ and $E > 8\varepsilon t$, we can change the order of the integrations under these conditions. Then we first integrate with respect to β in (3·25). Next applying the inverse Bessel transformations and integrating with respect to α, we get finally

$$\pi_2 = -\frac{1}{8\pi^4 i} \int\int\int_{-i\infty}^{+i\infty} ds dp dq \left(\frac{E_0}{E}\right)^s \frac{1}{E}\left(\frac{E}{E_s}\right)^2$$

$$\times \left(\frac{\varepsilon}{E}\right)^q \left(\frac{E^2 r^2}{E_s^2}\right)^{-p-1} \Gamma(p+1)\Gamma(-q)\mathfrak{M}_2(p, q, s, t). \tag{3.26}$$

The restrictions $E > \frac{E_s x t^{\frac{3}{2}}}{3}$ and $E > 8\varepsilon t$ can be dropped now, because (3·26) exists for any value of E and r. Now it can be stated that (3·26) is the exact solution of the differential lateral structure functions for any value of E and r derived by the principle of analytic continuation. The expression for the integral lateral structure function, $\Pi_2 (E_0, E, r, t)$, i.e. the lateral structure function for the electrons with energy larger than E, is obtained by the integration with respect to energy, and given by

$$\Pi_2(E_0, E, r, t) = -\frac{1}{8\pi^4 i} \int\int\int_{-i\infty}^{i\infty} \frac{ds dp dq}{s+2p+q} \left(\frac{E_0}{E}\right)^s \left(\frac{E}{E_s}\right)^2 \left(\frac{\varepsilon}{E}\right)^q \left(\frac{E^2 r^2}{E_s^2}\right)^{-p-1}$$

$$\times \Gamma(p+1)\Gamma(-q)\mathfrak{M}_2(p, q, s, t) \ . \tag{3.27}$$

At the limit for $E=0$, the integration with respect to q is equal to the residues of the integrands at $q=-s-2p$, and we have accurately

$$\Pi_2(E_0, 0, r, t) = -\frac{1}{4\pi^3}\int_{-i\infty}^{i\infty}\int ds\, dp\left(\frac{E_0}{\varepsilon}\right)^s\left(\frac{\varepsilon}{E_s}\right)^2\left(\frac{\varepsilon^2\gamma^2}{E_s^2}\right)^{-p-1}$$

$$\times\Gamma(p+1)\Gamma(s+2p)\mathfrak{M}_2(p,-s-2p,s,t)\,. \qquad (3\cdot28)$$

Total number of the electrons is now obtained by the integration of Π_2 with respect to r, and we find

$$\int_0^\infty \Pi_2(E_0, 0, r, t)\, 2\pi r\, dr = \frac{1}{2\pi i}\int ds\left(\frac{E_0}{\varepsilon}\right)^s\Gamma(s)\mathfrak{M}_2(0, -s, s, t)\,, \qquad (3\cdot29)$$

wihch is the same expression as that obtained by Snyder[13] in the one-dimensional shower theory.

Similar treatments are also possible for the analytical solutions of the structure functions for photons, which are sometimes important for the analysis of the spread of extensive air showers detected by the apparatus under a thick absorber. It can be shown easily from the equation (3·2), using the transformation (3·9), that

$$g(x, \zeta=0) = \lim_{(\xi-t)\to0}\int_0^t C'e^{-\sigma_0(t-t')}f(x, \zeta_1=x(\xi-t), \zeta_2=0)\, dt\,. \qquad (3\cdot30)$$

Similar expressions to (3·26), (3·27) and (3·28) are obtained for the differential and integral structure functions, γ_2 and Γ_2 respectively, for photons.

At the end of this section, we summarize the results satisfying various initial conditions.

B)　Analytical solutions.

(a)　Structure functions at depth t for the shower from a primary electron of energy E_0

(1)　Angular distribution functions for the electrons and photons

$$\pi_1(E_0, E, \theta, t) = -\frac{1}{8\pi^4 i}\int_{-i\infty}^{i\infty}\int\int ds\, dp\, dq\left(\frac{E_0}{E}\right)^s\frac{1}{E}\left(\frac{E}{E_s}\right)^2\left(\frac{\varepsilon}{E}\right)^q\left(\frac{E^2\theta^2}{E_s^2}\right)^{-p-1}$$

$$\times\Gamma(p+1)\Gamma(-q)\mathfrak{M}_1(p, q, s, t)\,, \qquad (3\cdot31)$$

$$\Pi_1(E_0, 0, \theta, t) = -\frac{1}{4\pi^3}\int_{-i\infty}^{i\infty}\int ds\, dp\left(\frac{E_0}{\varepsilon}\right)^{s'}\left(\frac{\varepsilon}{E_s}\right)^2\left(\frac{\varepsilon^2\theta^2}{E_s^2}\right)^{-p-1}$$

$$\times\Gamma(p+1)\Gamma(s+2p)\mathfrak{M}_1(p, -s-2p, s, t)\,, \qquad (3\cdot32)$$

where $\mathfrak{M}_1$ is given by

$$\left[\frac{\partial^2}{\partial t^2}+\left\{A(s+2p+q)+\sigma_0\right\}\frac{\partial}{\partial t}+A(s+2p+q)\sigma_0-B(s+2p+q)\right.$$

$$\left.\times C(s+2p+q)\right]\mathfrak{M}_1(p,q,s,t)$$

$$=\left(\frac{\partial}{\partial t}+\sigma_0\right)\{p\mathfrak{M}_1(p-1,q,s,t)+(s+2p+q)q\mathfrak{M}_1(p,q-1,s,t)\}$$

$$\tag{3.33}$$

with

$$\mathfrak{M}_1(0,0,s,t)=H_1(s)e^{\lambda_1(s)t}+H_2(s)e^{\lambda_2(s)t}. \tag{3.34}$$

$$\gamma_1(E_0,W,\theta,t)=-\frac{1}{8\pi^4i}\int\!\!\int\!\!\int_{-i\infty}^{i\infty}dsdpdq\left(\frac{E_0}{W}\right)^s\frac{1}{W}\left(\frac{W}{E_s}\right)^2\left(\frac{\varepsilon}{W}\right)^q\left(\frac{W^2\theta^2}{E_s}\right)^{-p-1}$$

$$\times\Gamma(p+1)\Gamma(-q)\mathfrak{M}_1'(p,q,s,t), \tag{3.35}$$

$$\Gamma_1(E_0,W,\theta,t)=-\frac{1}{8\pi^4i}\int\!\!\int\!\!\int_{-i\infty}^{i\infty}dsdpdq\frac{1}{s+2p+q}\left(\frac{E_0}{W}\right)^s\left(\frac{W}{E_s}\right)^2\left(\frac{\varepsilon}{W}\right)^q$$

$$\times\left(\frac{W^2\theta^2}{E_s^2}\right)^{-p-1}\Gamma(p+1)\Gamma(-q)\mathfrak{M}_1'(p,q,s,t), \tag{3.36}$$

where

$$\mathfrak{M}_1'(p,q,s,t)=\int_0^t C(s+2p+q)e^{-\sigma_0(t-t')}\mathfrak{M}_1(p,q,s,t)dt'. \tag{3.37}$$

(2) Lateral structure functions

The expressions for π_2, Π_2, γ_2 and Γ_2 are obtained by substituting γ, $\mathfrak{M}_2$, and $\mathfrak{M}_2'$ in θ, $\mathfrak{M}_1$, and $\mathfrak{M}_1'$ in the expressions for π_1, Π_1, γ_1 and Γ_1 respectively. Here

$$\mathfrak{M}_2(p,q,s,t)=\lim_{(\xi-t)\to0}M(p,q,s,t,\xi-t),$$

$$\mathfrak{M}_2'(p,q,s,t)=\int_0^t C(s+2p+q)e^{-\sigma_0(t-t')}M(p,q,s,t,t-t')dt',$$

and

$$\left[\frac{\partial^2}{\partial t^2}+\left\{A(s+2p+q)+\sigma_0\right\}\frac{\partial}{\partial t}+A(s+2p+q)\sigma_0-B(s+2p+q)\right.$$

$$\left.\times C(s+2p+q)\right]M(p,q,s,t,\xi-t)=$$

$$= \left(\frac{\partial}{\partial t} + \sigma_0\right)\Big\{ p(\xi - t)^2 M(p-1, q, s, t, \xi - t) + (s + 2p + q)$$

$$\times qM(p, q-1, s, t, \xi - t)\Big\} \tag{3.38}$$

with

$$M(0, 0, s, t, \xi - t) = H_1(s)e^{\lambda_1(s)t} + H_2(s)e^{\lambda_2(s)t}. \tag{3.39}$$

(b) Structure functions at depth t for the shower from a primary photon of energy W_0

(1) Angular structure functions

The expressions for $\pi_1(W_0)$, $\Pi_1(W_0)$, $r_1(W_0)$ and $\Gamma_1(W_0)$ are obtained by substituting W_0, $\mathfrak{N}_1$ and $\mathfrak{N}_1'$ in E_0, $\mathfrak{M}_1$ and $\mathfrak{M}_1'$ in the expressions (3.31), (3.32), (3.35) and (3.36). Here $\mathfrak{N}_1$ satisfies the same equation with $\mathfrak{M}_1$, but the boundary condition is given by

$$\mathfrak{N}_1(0, 0, s, t) = \frac{B(s)}{\lambda_1(s) - \lambda_2(s)}\{e^{\lambda_1(s)t} - e^{\lambda_2(s)t}\} \tag{3.40}$$

and

$$\mathfrak{N}_1'(p, q, s, t) = \int_0^t C(s + 2p + q)e^{-\sigma_0(t - t')}\mathfrak{N}_1(p, q, s, t)dt'$$

$$+ \lim_{\delta \to 0} \frac{\Gamma\left(p + \frac{1}{2}\right)}{\sqrt{\pi}\,\Gamma(p+1)}\delta^{-p+q}e^{-\sigma_0 t}. \tag{3.41}$$

(2) Lateral structure functions

The expressions for $\pi_2(W_0)$, $\Pi_2(W_0)$, $r_2(W_0)$ and $\Gamma_2(W_0)$ are obtained by substituting r, W_0, $\mathfrak{N}_2$ and $\mathfrak{N}_2'$ in θ, E_0, $\mathfrak{M}_1$ and $\mathfrak{M}_1'$ in the expressions (3.31), (3.32), (3.35) and (3.36). Here

$$\mathfrak{N}_2(p, q, s, t) = \lim_{(\xi - t) \to 0} N(p, q, s, t, \xi - t),$$

$$\mathfrak{N}_2'(p, q, s, t) = \int_0^t C(s + 2p + q)e^{-\sigma_0(t - t')}N(p, q, s, t, t - t')dt'$$

$$+ \lim_{\delta \to 0} \frac{\Gamma\left(p + \frac{1}{2}\right)}{\sqrt{\pi}\,\Gamma(p+1)}\delta^{-p+q}e^{-\sigma_0 t} \tag{3.42}$$

and $N(p, q, s, t, \xi - t)$ satisfies the equation (3.38). The boundary condition is given by

$$N(0, 0, s, t, \xi - t) = \frac{B(s)}{\lambda_1(s) - \lambda_2(s)}\Big\{e^{\lambda_1(s)t} - e^{\lambda_2(s)t}\Big\}.$$

Now as the analytical expressions for the structure functions are obtained under the various boundary conditions, all the problems concerning the spread of cascade showers can be treated within a limit of our approximations.

For instance, the expression of the structure function near the core can be derived easily from the above formulae by using the poles appearing the integrals with respect to p. Integration with respect to s is performed by the saddle point method. Then the structure functions near the core are given by

$$\left.\begin{array}{ll} \pi_2 \sim \dfrac{1}{r^{2-\bar{s}-\frac{2}{3}}} & \text{for} \quad 2-\bar{s}-\dfrac{2}{3}>0 \\[4mm] \pi_2 \sim \text{constant} & \text{for} \quad 2-\bar{s}-\dfrac{2}{3}<0 \end{array}\right\} \text{in Approximation A,} \tag{3·43}$$

where $\bar{s}$ is defined by the equation

$$\left.\dfrac{\partial \lambda_1(s)t}{\partial s}\right|_{\bar{s}}+\ln(E_0/E)+\ln(Er/E_s)=0, \tag{3·44}$$

$$\left.\begin{array}{ll} \Pi_2 \sim \dfrac{1}{r^{2-\bar{s}}} & \text{for} \quad 2-\bar{s}>0 \\[4mm] \Pi_2 \sim \text{constant} & \text{for} \quad 2-\bar{s}<0 \end{array}\right\} \text{in Approximation B} \tag{3·45}$$

with

$$\left.\dfrac{\partial \lambda_1(s)t}{\partial s}\right|_{\bar{s}}+\ln(E_0/\varepsilon)+\ln(\varepsilon r/E_s)=0, \tag{3·46}$$

$$\left.\begin{array}{ll} \gamma_2 \sim \dfrac{1}{r^{2-\bar{s}}} & \text{for} \quad 2-\bar{s}>0 \\[4mm] \gamma_2 \sim \text{constant} & \text{for} \quad 2-\bar{s}<0 \end{array}\right\} \text{in Approximation A} \tag{3·47}$$

with

$$\left.\dfrac{\partial \lambda_1(s)t}{\partial s}\right|_{\bar{s}}+\ln(E_0/E)+\ln(Er/E_s)=0, \tag{3·48}$$

$$\left.\begin{array}{ll} \Gamma_2 \sim \dfrac{-\ln r}{r^{2-\bar{s}}} & \text{for} \quad 2-\bar{s}>0 \\[4mm] \Gamma_2 \sim \text{constant} & \text{for} \quad 2-\bar{s}<0 \end{array}\right\} \text{in Approximation B} \tag{3·49}$$

with

$$\left.\dfrac{\partial \lambda_1(s)t}{\partial s}\right|_{\bar{s}}+\ln(E_0/\varepsilon)+\ln(\varepsilon r/E_s)=0, \tag{3·50}$$

At the limit for $E_0 \to \infty$, all s's here defined agree with the shower age usually used in the one-dimensional shower theory. The behavior of the structure function near the core derived by Molière, Pomeranchuk and Migdal[14] can be said to be included in the above formulae as the particular cases and further details of our functions near the core will be discussed in Appendix III.

C) Numerical results.

Since we are most interested in the integral structure function of electrons, the method of evaluation of the complex intergral (3·27) is shown as an example. Similar treatments are also possible for the evaluation of other structure functions.

It is sometimes convenient to introduce the normalized structure function, which is defined by

$$P_{\Pi_2}(E_0, 0, r, t) = \frac{\Pi_2}{\int_0^\infty \Pi_2 2\pi r \, dr} \, , \tag{3·51}$$

so that

$$\int_0^\infty P_{\Pi_2}(E_0, 0, r, t) 2\pi r \, dr = 1 \, . \tag{3·52}$$

It follows from (3·28) and (3·29) that

$$P_{\Pi_2}(E_0, 0, r, t)$$

$$= \frac{\dfrac{1}{2\pi^2 i} \displaystyle\int_{-i\infty}^{i\infty}\!\!\int ds \, dp \left(\dfrac{E_0}{\varepsilon}\right)^s \left(\dfrac{\varepsilon}{E_s}\right)^2 \left(\dfrac{\varepsilon^2 r^2}{E_s^2}\right)^{-p-1} \Gamma(p+1)\Gamma(s+2p)\mathfrak{M}_2(p, -s-2p, s, t)}{\displaystyle\int_{-i\infty}^{i\infty} ds \left(\dfrac{E_0}{\varepsilon}\right)^s \Gamma(s)\mathfrak{M}_2(0, -s, s, t)} \, . \tag{3·53}$$

For the sake of simplicity, here we treat a limiting case in which $E_0/\varepsilon \to \infty$. In this case, the integral with respect to s can be carried out by the saddle point method independent of the integral with respect to p. Hence, (3·53) becomes

$$P_{\Pi_2}(\infty, 0, r, t)$$

$$= \frac{\dfrac{1}{2\pi^2 i} \displaystyle\int_{-i\infty}^{i\infty} dp \left(\dfrac{\varepsilon}{E_s}\right)^2 \left(\dfrac{\varepsilon^2 r^2}{E_s^2}\right)^{-p-1} \Gamma(p+1)\Gamma(\bar{s}+2p)\mathfrak{M}_2(p, -\bar{s}-2p, \bar{s}, t)}{\Gamma(\bar{s})\mathfrak{M}_2(0, -\bar{s}, \bar{s}, t)} \, , \tag{3·54}$$

where $\bar{s}$ is the shower age and is defiend by

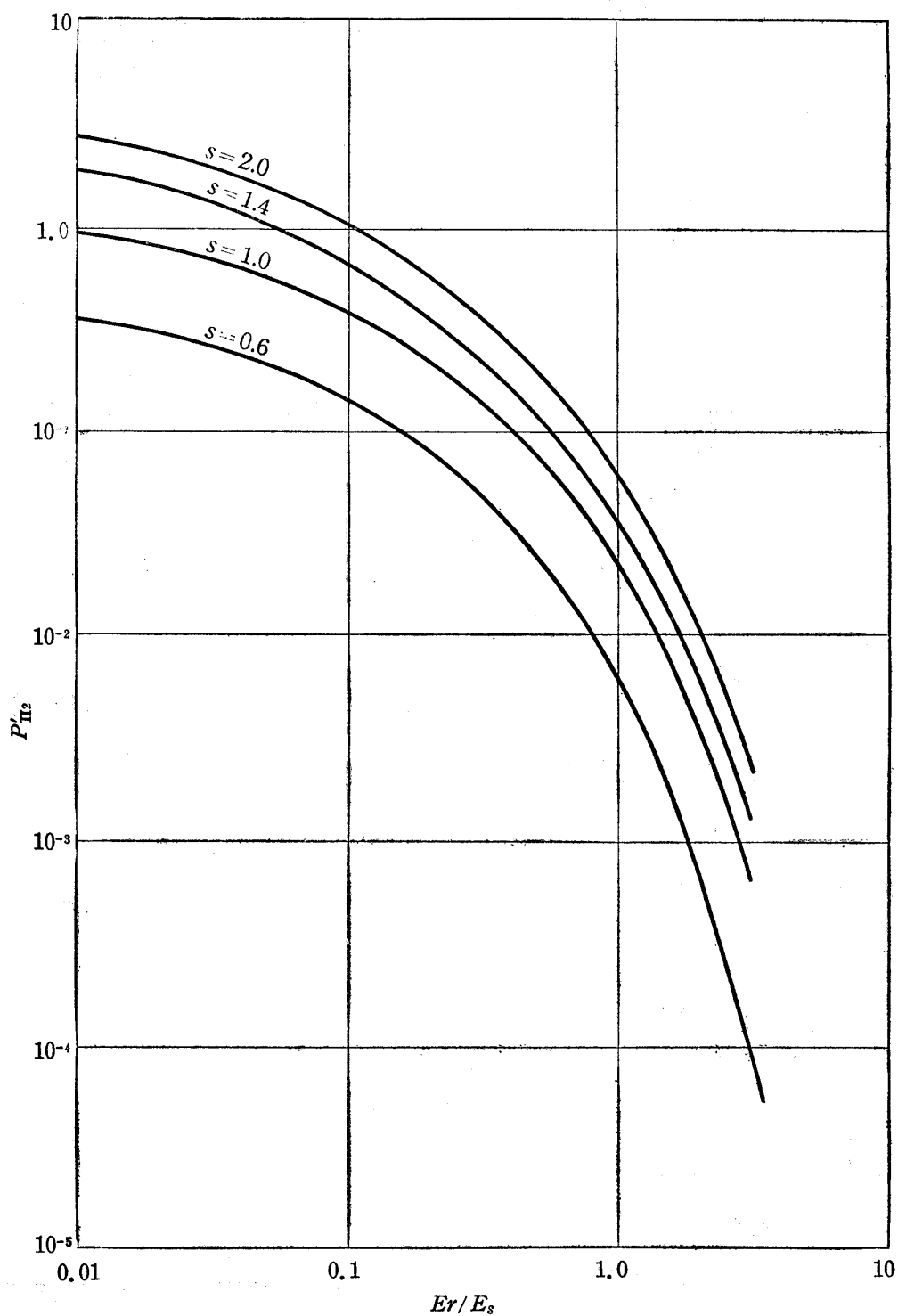$$\ln(E_0/\varepsilon) + \lambda_1(\bar{s})t = 0 \, . \tag{3·55}$$

Fig. 1. Normalized integral structure functions, $\left(\dfrac{E\gamma}{E_s}\right)^{s-2} P'_{\Pi2}$, at a few different ages in the approximation A. (See Table 1, p. 113.)

$P'_{\Pi2}$ is normarized as

$$\int_0^\infty \left(\frac{E\gamma}{E_s}\right)^{s-2} P'_{\Pi2} 2\pi \left(\frac{E\gamma}{E_s}\right) d\left(\frac{E\gamma}{E_s}\right) = 1 ,$$

The integral with respect to p can also be evaluated by the saddle point method. Writing

$$e^{u(\bar{s},\,p,\,t)} = \Gamma(p+1)\Gamma(s+2p)\mathfrak{M}_2(p,\ -\bar{s}-2p,\ \bar{s},\ t)\,, \tag{3.56}$$

the saddle point $\bar{p}$ is determined by the equation

$$-2\ln(\varepsilon r/E_s) + \frac{\partial u(s,\,p,\,t)}{\partial p} = 0\,.$$

Then we get

$(r/r_1)^{2-s}P_{\mathrm{II}_2}$
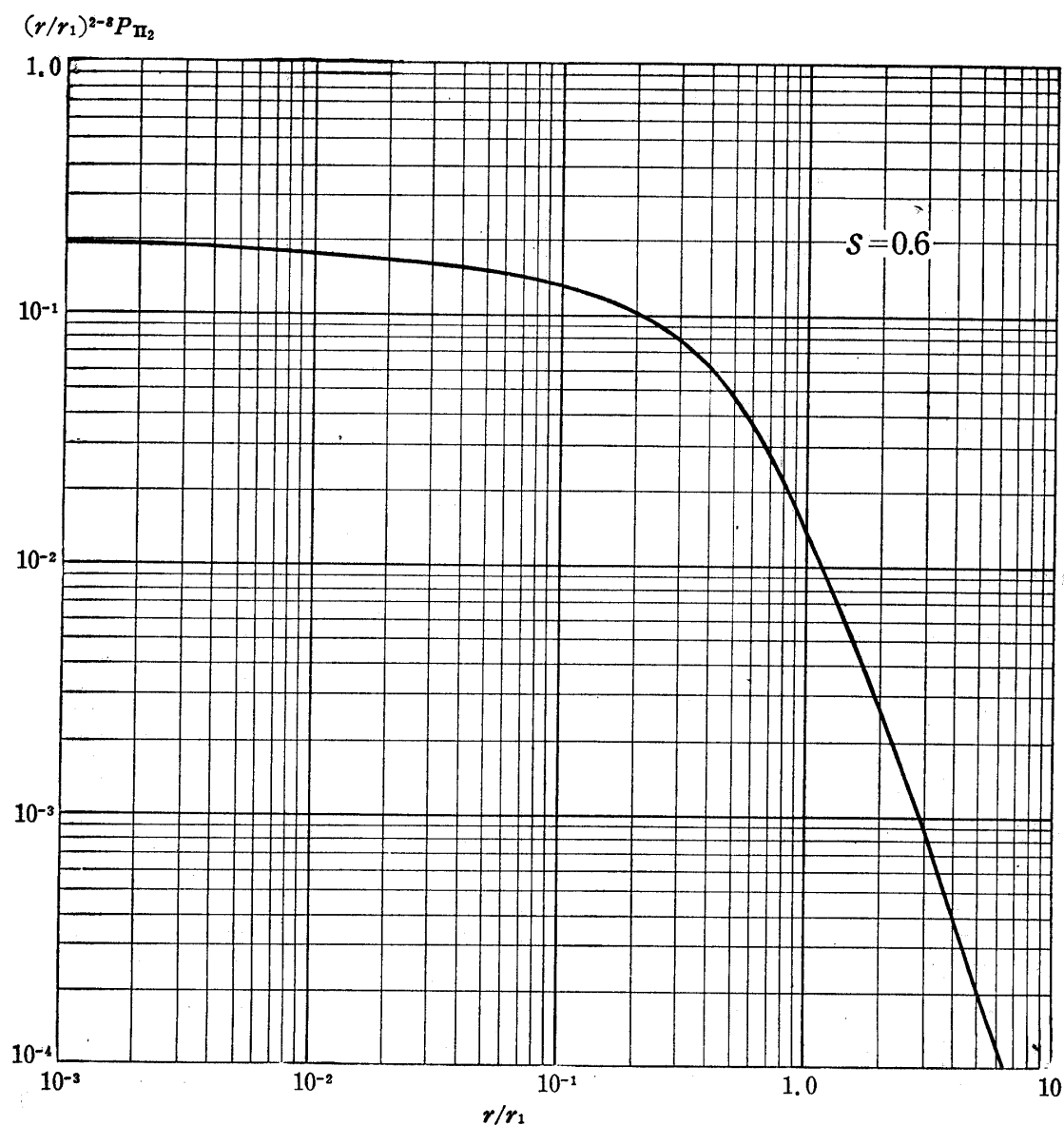

Distance from the shower axis in Molière units

Fig. 2. Normalized Lateral Structure Function for $s=0.6$ in Approximation B. Molière unit is $r_1 = E_s/\varepsilon$ cascade units.

$$P_{\Pi_2}(\infty,0,r,t) = \frac{1}{\pi\sqrt{2\pi u''(\bar{s},\bar{p},t)}}\frac{\left(\dfrac{\varepsilon}{E_s}\right)^2\left(\dfrac{\varepsilon^2\gamma^2}{E_s^2}\right)^{-\bar{p}-1}e^{u(\bar{s},\bar{p},t)}}{\Gamma(\bar{s})\mathfrak{M}(0,-\bar{s},\bar{s},t)}. \quad (3\cdot57)$$

Since $\dfrac{\mathfrak{M}_2(p,-\bar{s}-2p,\bar{s},t)}{\mathfrak{M}_2(0,-\bar{s},\bar{s},t)}$ and $\dfrac{\partial u}{\partial p}$ do not explicitly depend on "t" as shown in Appendix IV, it may be convenient to express the structure function by $P_{\Pi_2}(\infty,0,r,\bar{s})$ instead of the expression $P_{\Pi_2}(\infty,0,r,t)$.

The numerical results of the normalized distribution functions are presented in Tables 1 and 2, and the behaviour of the integral structure
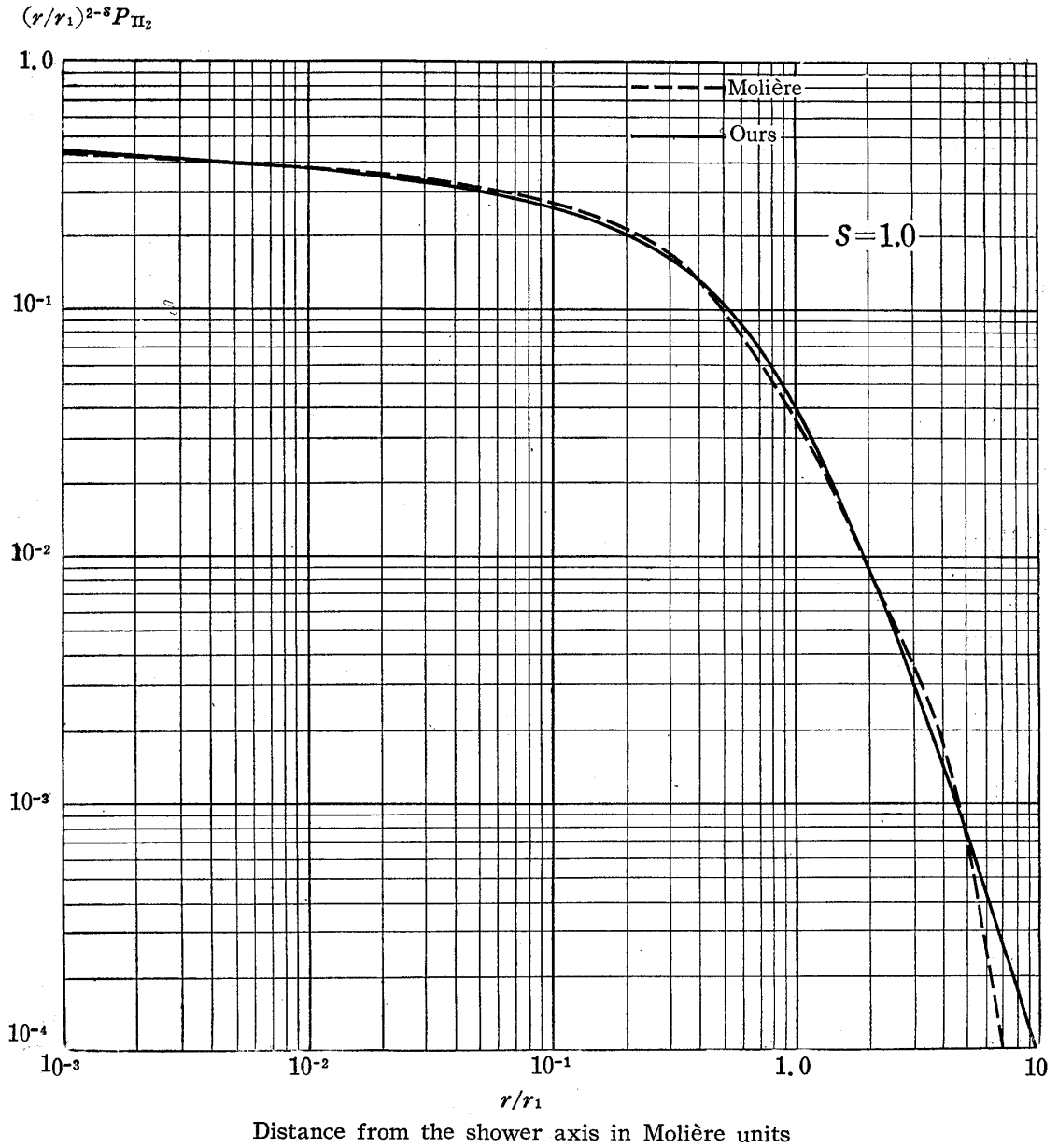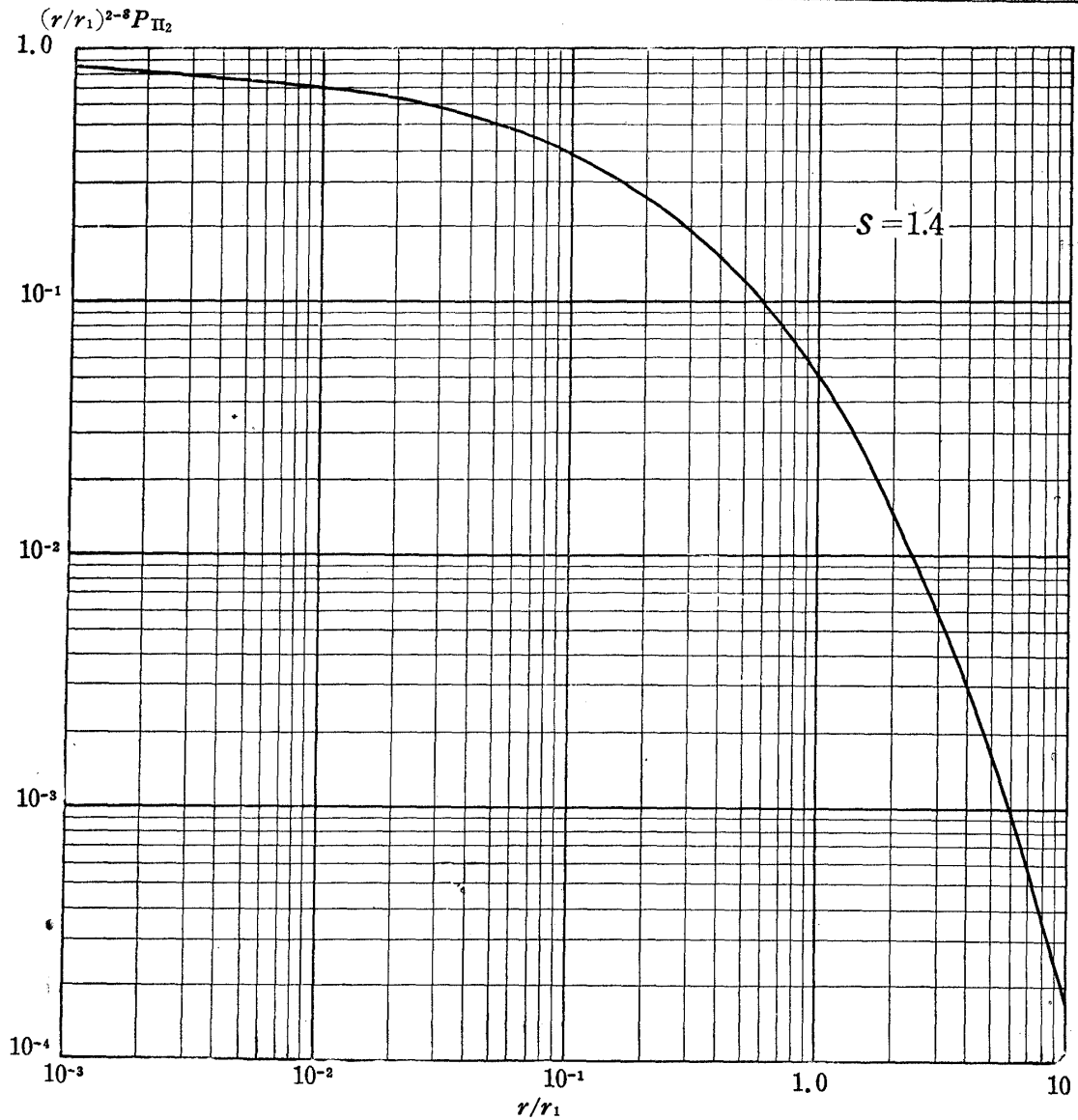

Fig. 3. Normalized Lateral Structure Function for $s=1.0$ in Approximation B.

Table 1.

Integral Structure Functions P'_{Π_2} of Electrons in the Approximation A. P'_{Π_2} is defined by $P'_{\Pi_2}=\left(\frac{Er}{E_s}\right)^{2-s}P_{\Pi_2}$, and is normalized as $\int_0^\infty\left(\frac{Er}{E_s}\right)^{s-2}P'_{\Pi_2}2\pi\left(\frac{Er}{E_s}\right)d\left(\frac{Er}{E_s}\right)=1$.

Er/E_s	0	0.01	0.03	0.1	0.3	1.0	3.0
$P'_{\Pi_2}(s=0.6)$	0.38	0.34	0.27	0.17	0.05	0.0044	0.00009
$P'_{\Pi_2}(s=1.0)$	1.01	0.91	0.70	0.37	0.15	0.019	0.00065
$P'_{\Pi_2}(s=1.4)$	2.5	1.9	1.35	0.68	0.27	0.041	0.0019
$P'_{\Pi_2}(s=2.0)$	$\lim_{\frac{r}{r_1}\to 0}\left(-0.53\times\ln\frac{Er}{E_s}\right)$	2.5	1.8	0.99	0.37	0.60	0.37

$(r/r_1)^{2-s}P_{\Pi_2}$

$S=1.4$

r/r_1

Distance from the shower axis in Molière units

Fig. 4. Normalized Lateral Structure Function for $s=1.4$ in Approximation B.

functions for a few different shower ages are shown in Figs. 1, 2, 3, 4, and 5 comparing with the Molière function.

$(r/r_1)^{2-s} P_{\Pi_2}$

r/r_1
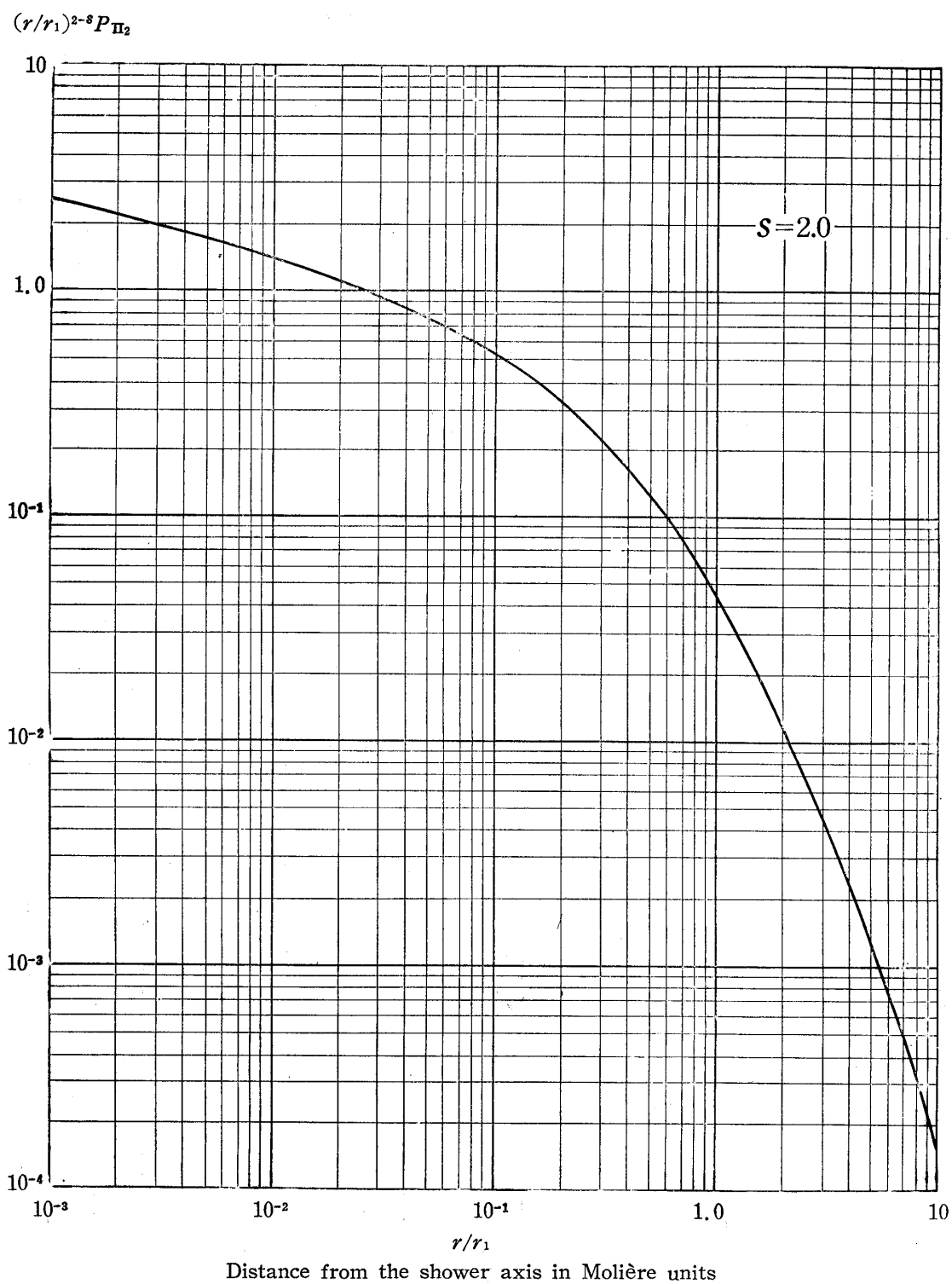
Distance from the shower axis in Molière units

Fig. 5. Normalized Lateral Structure Function for $s=2.0$ in Approximation B.

Table 2.

The Normalized Lateral Structure Function $(r/r_1)^{2-s}P_{\Pi2}(r/r_1, s)$ for $s=0.6$, 1.0, 1.4, and 2.0 in Approximation B, where $r_1=E_s/\varepsilon$ cascade units.

r/r_1 \ s	$(r/r_1)^{2-s}P_{\Pi2}(r/r_1, s)$
	0.6	1.0	1.4	2.0
0.001	$1.95 \cdot 10^{-1}$	$4.4 \cdot 10^{-1}$	$8.5 \cdot 10^{-1}$	2.4
0.003	$1.90 \cdot 10^{-1}$	$4.2 \cdot 10^{-1}$	$8.0 \cdot 10^{-1}$	1.92
0.01	$1.81 \cdot 10^{-1}$	$3.9 \cdot 10^{-1}$	$7.1 \cdot 10^{-1}$	1.40
0.03	$1.58 \cdot 10^{-1}$	$3.4 \cdot 10^{-1}$	$5.8 \cdot 10^{-1}$	$9.3 \cdot 10^{-1}$
0.1	$1.34 \cdot 10^{-1}$	$2.65 \cdot 10^{-1}$	$3.8 \cdot 10^{-1}$	$5.3 \cdot 10^{-1}$
0.2	$1.08 \cdot 10^{-1}$	$2.03 \cdot 10^{-1}$	$2.6 \cdot 10^{-1}$	$3.2 \cdot 10^{-1}$
0.5	$4.9 \cdot 10^{-2}$	$1.09 \cdot 10^{-1}$	$1.22 \cdot 10^{-1}$	$1.21 \cdot 10^{-1}$
1.0	$1.35 \cdot 10^{-2}$	$4.1 \cdot 10^{-2}$	$5.0 \cdot 10^{-2}$	$4.4 \cdot 10^{-2}$
2.0	$2.64 \cdot 10^{-3}$	$8.8 \cdot 10^{-3}$	$1.48 \cdot 10^{-3}$	$1.18 \cdot 10^{-2}$
5.0	$2.16 \cdot 10^{-4}$	$7.7 \cdot 10^{-4}$	$1.55 \cdot 10^{-4}$	$1.32 \cdot 10^{-3}$

§4. Structure Function without the Landau Approximation

In the preceding section, we were limited only to the structure function in the Landau approximation. In the Landau approximation higher moments of the Rutherford cross section are all neglected. Thus the contributions of plural and single scattering are not included in this approximation, and the structure function thus derived will seriously be in error at the tail of the structure function.

The approximation made in the Williams theory[9] for the multiple scattering of a single charged particle just corresponds to this Landau approximation, in which Williams obtained the wellknown Gaussian distribution for the lateral and the angular structure functions. The function, however, does not agree with the exact one which is obtained without the Landau approximation not only at the tail of the distribution function but even in the small angle region.[15]

Similar deviations have also been found in the angular structure function of the electron shower which was obtained by Chartres and Messel[2] without using the Landau approximation. Their treatment, is however, limited to the angular structure function at the shower maximum in the approximation A.

In this section, a theory without use of the Landau approximation is formulated, in which the contributions of the single and plural scattering are included. The treatment is based on Molière's[15] scattering theory for

a single charged particle.

As was shown in §2, the variation in the number of shower particles in the interval $(\theta, d\theta)$ by scattering is given by

$$\int_{-\infty}^{+\infty} \sigma(\theta-\theta')\pi(\theta')d\theta' - \int_{-\infty}^{+\infty} \sigma(\theta')\pi(\theta)d\theta'. \qquad (4\cdot1)$$

Multiplying $e^{i(\zeta\theta)}$ by the expression $(4\cdot1)$ and integrating it with respect to θ from 0 to ∞, we get

$$-\int_0^\infty J_0(\zeta\theta)\pi(\theta)\theta d\theta \int_0^\infty [1-J_0(\zeta\theta)]\sigma(\theta')2\pi\theta'd\theta', \qquad (4\cdot2)$$

where we have made use of the symmetry property of $\pi(\theta)$ around the shower axis. As has been shown in §2, the scattering probability is approximately given by the formula

$$\frac{1}{4\pi\ln(181Z^{-1/3})}\left(\frac{E_s}{E}\right)^2\frac{d\theta}{\theta^4}$$

within the region between $\theta_{\min}$ and $\theta_{\max}$.

As in Molière's theory, we now take into account only the screening effect by the outer electrons, and divide the integral, $(4\cdot2)$, in the following two parts:

$$\int_0^\infty \sigma(\theta)[1-J_0(\zeta\theta)]\theta d\theta = \int_{\theta_0}^\infty + \int_0^{\theta_0}, \qquad (4\cdot3)$$

where θ_0 is an angle of the order of $\theta_{\min}$. The first terms of the right-hand side of $(4\cdot3)$ can be integrated by parts and gives;

$$\int_{\theta_0}^\infty \frac{1}{2\ln(181Z^{-1/3})}\left(\frac{E_s}{E}\right)^2\frac{1}{\theta^3}[1-J_0(\zeta\theta)]d\theta$$

$$= \frac{1}{2\ln(181Z^{-1/3})}\left(\frac{E_s\zeta}{E}\right)^2\int_{\zeta\theta_0}^\infty [1-J_0(y)]\frac{dy}{y^3}$$

$$= \frac{1}{8\ln(181Z^{-1/3})}\left(\frac{E_s\zeta}{E}\right)^2\left[\frac{2}{(\zeta\theta_0)^2}\{1-J_0(\zeta\theta_0)\}\right.$$

$$\left. +\frac{J(\zeta\theta_0)}{\zeta\theta_0}+\int_{\zeta\theta_0}^\infty \frac{J_0(y)}{y}dy\right]$$

$$= \frac{1}{8\ln(181Z^{-1/3})}\left(\frac{E_s\zeta}{E}\right)^2[1+\ln2-\ln\zeta\theta_0-c+O\{(\zeta\theta_0)^2\}], \qquad (4\cdot4)$$

where $c=0.577\ldots$ is Euler's constant.

For the second term in $(4\cdot3)$, Molière put

$$\int_0^{\theta_0} \sigma(\theta) 2\pi\theta d\theta [1 - J_0(\zeta\theta)] = \frac{\pi\zeta^2}{2} \int_0^{\theta_0} \theta^2 \sigma(\theta)\theta d\theta$$

$$= \frac{1}{8\ln(181Z^{-1/3})} \left(\frac{E_s\zeta}{E}\right)^2 \left[-\ln X_a + \ln\theta_0 - \frac{1}{2}\right]. \qquad (4\cdot5)$$

For the actual determination of X_a, Molière obtained this value by using the scattering cross section for the Tomas-Fermi potential. Then, he gets

$$X_a^2 = \theta^2{}_{\min}(1.13 + 3.76\alpha^2), \qquad (4\cdot6)$$

where α is the well-known parameter,

$$\alpha = Ze^2/\hbar c.$$

Then from $(4\cdot2)$, $(4\cdot3)$, $(4\cdot4)$ and $(4\cdot5)$, we get

$$\int_{\cdot}^{\infty} = \frac{1}{8\ln(181Z^{-1/3})} \frac{E_s^2\zeta^2}{E^2} \left[\frac{1}{2} + \ln 2 - c - \ln(X_a\zeta)\right]$$

$$= \frac{E_s'^2\zeta^2}{4E^2} \left[b - \ln\frac{E_s'^2\zeta^2}{4E^2}\right], \qquad (4\cdot7)$$

where
$$E_s' = \frac{E_s}{2(\ln 181 Z^{-1/3})^{1/2}} \qquad (4\cdot8)$$

and
$$b = 1 - 2c - \ln\left(\frac{X_a E}{E_s'}\right)^2. \qquad (4\cdot9)$$

As can be easily proved, $(E_s'/X_a E)^2$ is the approximate number of collisions of an electron passing through the matter of thickness of one cascade unit, and then b is approximately equal to its logarithm. Furthermore, as X_a is inversely proportional to E, $X_a E$ in the formula $(4\cdot9)$ is independent of E, and b is only the function of the traversing material.

Now, as done in Molière's theory, we introduce a new parameter, Ω, defined by

$$\Omega - \ln \Omega = b.$$

Then the formula $(4\cdot7)$ becomes:

$$\frac{K^2\zeta^2}{4E^2} \left(1 - \frac{1}{\Omega}\ln\frac{K^2\zeta^2}{4E^2}\right), \qquad (4\cdot10)$$

where we put

$$K = \Omega^{1/2}E_s'.$$

Then the diffusion equation of the structure functions without use of the Landau approximation is given only by replacing $\dfrac{E_s^2\zeta^2}{4E^2}$ by

$$\frac{K^2\zeta^2}{4E^2}\left[1-\frac{1}{\varOmega}\ln\frac{K^2\zeta^2}{4E^2}\right] \text{ in the equation (3·5), and}$$

$$\left\{\left(\frac{\partial}{\partial t}-x\frac{\partial}{\partial \zeta}\right)^2+\left(A'+\sigma_0\right)\left(\frac{\partial}{\partial t}-x\frac{\partial}{\partial \zeta}\right)+\left(A'\sigma_0-B'C'\right)\right\}f(x,\zeta)$$

$$=\left(\frac{\partial}{\partial t}-x\frac{\partial}{\partial \zeta}+\sigma_0\right)\left\{-\frac{K^2\zeta^2}{4E^2}\left(1-\frac{1}{\varOmega}\ln\frac{K^2\zeta^2}{4E^2}\right)+\varepsilon\frac{\partial}{\partial E}\right\}f(x,\zeta). \quad (4·11)$$

This is the basic equation for the structure function without the Landau approximation, and the numerical values of K and $\varOmega$ for the several traversing materials are shown in Table 3.

<div align="center">Table 3.</div>

materials	C	Al	Fe	Pb	G₅ Emulsion	Air
Z	6	13	26	82		
K (MeV)	19. 2	19. 4	19. 5	19. 1	19. 7	19. 3
$\varOmega$	15. 4	14. 9	14. 3	12. 9	14. 0	15. 2

The solution of the equation (4·11) can now be obtained in the similar way as in the preceding section. As an example, we present here the derivation of the angular structure function in the approximation A.

Putting $\varepsilon=0$ and $x=0$ in equation (4·11), we get

$$L'f=-\frac{K^2\zeta^2}{4E^2}\left(1-\frac{1}{\varOmega}\ln\frac{K^2\zeta^2}{4E^2}\right)f, \quad (4·12)$$

where f is the Bessel transform of the angular structure function, and

$$L'=\frac{1}{\dfrac{\partial}{\partial t}+\sigma_0}\left[\frac{\partial^2}{\partial t^2}+\left(A'+\sigma_0\right)\frac{\partial}{\partial t}+\left(A'\sigma_0-B'C'\right)\right]. \quad (4·13)$$

As we did in §3, we first put

$$f=\frac{1}{4\pi i}\int_{-i\infty}^{+i\infty}\left(\frac{E_0}{E}\right)^s\frac{ds}{E}\sum_{n=0}^{\infty}\sum_{m=0}^{\infty}(-)^n\left(\frac{K^2\zeta^2}{4E^2}\right)^{n+m}\left(\frac{1}{\varOmega}\ln\frac{K^2\zeta^2}{4E^2}\right)^m\psi_{n,\,m},$$

$$(4·14)$$

and substitute the above formula in (4·12).

Since

$$\left(\frac{K^2\zeta^2}{4E^2}\right)^{n+m}\left(\frac{1}{\varOmega}\ln\frac{K^2\zeta^2}{4E^2}\right)^m=\left(\frac{1}{\varOmega}\frac{\partial}{\partial n}\right)^m\left(\frac{K^2\zeta^2}{4E^2}\right)^{n+m},$$

$$L'\frac{(-)^n}{E^{s+1}}\left(\frac{K^2\zeta^2}{4E^2}\right)^{n+m}\left(\frac{1}{\varOmega}\ln\frac{K^2\zeta^2}{4E^2}\right)^m\psi_{n,\,m}=$$

$$= \left(-\frac{1}{\Omega}\frac{\partial}{\partial n'} \right)^m L' \frac{1}{E^{s+1}} \left(\frac{-K^2\zeta^2}{4E^2} \right)^{n'+m} \psi_{n,m} \Big|_{n'=n}$$

$$= \frac{1}{E^{s+1}} \left(\frac{-K^2\zeta^2}{4E^2} \right)^{n+m} \left(-\frac{1}{\Omega} \right)^m \left(\frac{\partial}{\partial n'} + \ln\frac{K^2\zeta^2}{4E^2} \right)^m L(s+2n'+2m) \Big|_{n'=n} \psi_{n,m}$$

$$= \frac{1}{E^{s+1}} \left(\frac{-K^2\zeta^2}{4E^2} \right)^{n+m} \left(-\frac{1}{\Omega} \right)^m \sum_{l=0}^{m} {}_mC_l \left(\ln\frac{K^2\zeta^2}{4E^2} \right)^l \left(\frac{\partial}{\partial n'} \right)^{m-l} L(s+2n'+2m) \Big|_{n'=n} \psi_{n,m} ,$$

$$(4\cdot15)$$

where

$$L(s+2n+2m) = \frac{1}{\frac{\partial}{\partial t}+\sigma_0} \left(\frac{\partial}{\partial t} + \lambda_1(s+2n+2m) \right) \left(\frac{\partial}{\partial t} + \lambda_2(s+2n+2m) \right).$$

Putting $n+m=N$ and $\left(\dfrac{\partial}{\partial n'} \right)^{m-l} L(s+2n'+2m) = L^{(m-l)}$, $(4\cdot15)$ can be written as

$$\sum_{m=0}^{\infty} \sum_{N=m}^{\infty} \sum_{l=0}^{m} \left(\frac{1}{E} \right)^{s+1} \left(\frac{-K^2\zeta^2}{4E^2} \right)^{N} \left(-\frac{1}{\Omega} \right)^m {}_mC_l \left(\ln\frac{K^2\zeta^2}{4E^2} \right)^l L^{(m-l)} \psi_{N-m,m} . \quad (4\cdot16)$$

Now we change the order of the triple summations appearing in the above formula. As

$$\sum_{m=0}^{\infty} \sum_{N=m}^{\infty} \sum_{l=0}^{m} = \sum_{N=0}^{\infty} \sum_{m=0}^{N} \sum_{l=0}^{m} = \sum_{N=0}^{\infty} \sum_{l=0}^{N} \sum_{m=l}^{N} ,$$

the formula $(4\cdot16)$ becomes

$$\sum_{n=0}^{\infty} \sum_{l=0}^{N} \sum_{m'=0}^{N-l} \left(\frac{1}{E} \right)^{s+1} \left(-\frac{K^2\zeta^2}{4E^2} \right)^{N} \left(-\frac{1}{\Omega} \right)^{m'+l} {}_{m'+l}C_l \left(\ln\frac{K^2\zeta^2}{4E^2} \right)^l L^{(m')} \psi_{N-m'-l,\,m'+l} ,$$

$$(4\cdot17)$$

where we have replaced $m-l$ by m'. Comparing the formula $(4\cdot17)$ with the right-hand side of the equation $(4\cdot12)$ and equating the coefficients multiplied by the products of respective powers of $\dfrac{K^2\zeta^2}{4E^2}$ and $\ln\left(\dfrac{K^2\zeta^2}{4E^2} \right)$, we get the relation:

$$\sum_{n=0}^{N-l} \left(-\frac{1}{\Omega} \right)^n {}_{n+l}C_l L^{(n)} \psi_{N-n-l,\,n+l}$$

$$= \psi_{N-l-1,\,l} + \psi_{N-l,\,l-1} . \qquad (4\cdot18)$$

Now, we write the series solution, $(4\cdot14)$, as

$$f = \frac{1}{4\pi^2 i} \int_{-i\infty}^{i\infty} \left(\frac{E_0}{E} \right)^s \frac{ds}{E} \int\!\!\int_0^{\infty} d\alpha\, d\beta\, e^{-\alpha\frac{K^2\zeta^2}{4E^2} + \frac{\beta}{\Omega}\frac{K^2\zeta^2}{4E^2}\ln\frac{K^2\zeta^2}{4E^2}} F(\alpha,\beta),$$

$$(4\cdot19)$$

and put the Mellin transform of $F(\alpha, \beta)$ as $\mathfrak{M}_1(p, u)$. Then, since

$$\mathfrak{M}_1(p, u) = \int\!\!\int_0^\infty \alpha^p \beta^u F(\alpha, \beta) d\alpha d\beta,$$

we get the relation

$$\Gamma(p+1)\Gamma(u+1)\psi_{p,u} = \mathfrak{M}_1(p, u), \tag{4.20}$$

by equating the formula (4·14) to (4·19).

The difference equation difining $\mathfrak{M}_1(p, u)$ is

$$\sum_{n=0}^\infty {}_N C_n \left(-\frac{1}{\Omega}\right)^n L^{(n)}(s+2p+2u)\mathfrak{M}_1(p-n, u+n)$$

$$= p\,\mathfrak{M}_1(p-1, u) + u\,\mathfrak{M}_1(p, u-1), \tag{4.21}$$

with appropriate initial conditions for $\mathfrak{M}(0,0)$, which is easily obtained by substituting the formula (4·20) in (4·18).

The inverse Bessel transformation is made as follows. First, we make use of the relations of the inverse Mellin transformation:

$$F(\alpha, \beta) = -\frac{1}{4\pi^2} \int\!\!\int_{-i\infty}^{+i\infty} dp\,du \frac{\mathfrak{M}_1(p, u)}{\alpha^{p+1}\beta^{u+1}}. \tag{4.22}$$

Substituting the above relation in (4·19) and expanding $e^{-\alpha\frac{K^2\zeta^2}{4E^2}}$ $+\frac{\beta}{\Omega}\frac{K^2\zeta^2}{4E^2}\ln\frac{K^2\zeta^2}{4E^2}$ into the power series of $\frac{1}{\Omega}$ as

$$e^{-\alpha\frac{K^2\zeta^2}{4E^2}} \sum_{n=0}^\infty \frac{1}{n!}\left(\frac{1}{\Omega}\right)^n \left(\beta\frac{K^2\zeta^2}{4E^2}\ln\frac{K^2\zeta^2}{4E^2}\right)^n, \tag{4.23}$$

we perform the inverse Bessel transformation.

Then we get the angular structure function

$$\pi_1 = \pi_1^{(0)} + \frac{1}{\Omega}\pi_1^{(1)} + \frac{1}{\Omega^2}\pi_1^{(2)} + \cdots, \tag{4.24}$$

where

$$\pi_1^{(0)} = -\frac{1}{4\pi^3}\int\!\!\int_{-i\infty}^{i\infty} ds\,dp \left(\frac{E_0}{E}\right)^s \frac{1}{E}\left(\frac{E}{K}\right)^2 \left(\frac{E^2\theta^2}{K^2}\right)^{-p-1} \Gamma(p+1)\mathfrak{M}_1(p, 0, s, t), \tag{4.25}$$

and

$$\pi_1^{(1)} = \frac{1}{4\pi^3}\int\!\!\int_{-i\infty}^{i\infty} ds\,dp \left(\frac{E_0}{E}\right)^s \left(\frac{1}{E}\right)\left(\frac{E}{K}\right)^2 \left(\frac{E^2\theta^2}{K^2}\right)^{-p-2} \Gamma(p+2)(p+1) \times$$

$$\times \left\{ \psi(p+2) + \psi(-p-1) - \ln\frac{E^2\theta^2}{K^2} \right\} \mathfrak{M}_1(p, 1, s, t). \qquad (4 \cdot 26)$$

The series solution, $(4 \cdot 24)$, just corresponds to the one given by Molière in his scattering theory for a single charged particle.

As in Molière's theory, the first term of the series $(4 \cdot 24)$, i.e., $\pi^{(0)}$, represents the spread by multiple scattering of electrons when they are traversing the matter, and in fact it is just the same function as the solution $(3 \cdot 31)$ derived under the Landau approximation except for the slight differences in the definitions of K and $\mathfrak{M}$.

The second term of the series, $(4 \cdot 24)$, is the contribution by the single scattering and some of the plural scattering. Thus it gives a less contribution than $\pi^{(0)}$ near the shower axis ($1/\Omega$ times smaller than $\pi^{(0)}$), but it predominates at the tail of the structure function. At a large distance from the shower axis, $\pi^{(1)}$ can be developed in a series of power of $1/\theta$.

Integration in $(4 \cdot 26)$ with respect to p is carried out under the condition of $\dfrac{E\theta}{K} \gg 1$, using the poles of $(p+1)\psi(-p-1)$ at $p=0, 1, 2, \cdots$, and the formula becomes;

$$\pi_1^{(1)} = \frac{1}{2\pi^2 i} \int_{-i\infty}^{i\infty} ds \left(\frac{E_0}{E}\right)^s \frac{1}{E} \left\{ \Gamma(2)\left(\frac{E^2\theta^2}{E_s^2}\right)^{-2} \mathfrak{M}_1(0, 1, s, t) \right.$$

$$\left. + 2\Gamma(3)\left(\frac{E^2\theta^2}{E_s^2}\right) \mathfrak{M}_1(1, 1, s, t) + \cdots \right\}. \qquad (4 \cdot 27)$$

The first term of the above series represents the effect by the single scattering, and gives just the same function as that obtained by Eyges[16] in his genious theory for the calculation of the effect by the single scattering in an electron shower.

A similar argument can also be made for the lateral structure function. In this case we have only to replace θ and $\mathfrak{M}_1$ by r and $\mathfrak{M}_2$ respectively in which the definition of $\mathfrak{M}_2$ is shown at the end of this section.

Numerical calculations of the integrals in the formula $(4 \cdot 24)$ are carried out, and it can be proved that the series $(4 \cdot 24)$ converges very rapidly. Summation up to the second term is sufficient for the practical applications as in Molière's theory. Numerical results are shown in Fig. 6 comparing with those obtained in other theories.

The other structure functions, such as the lateral structure function in the approximation B, can be obtained in the similar way as shown above.

At the end of this section, we summarize the analytical solutions for the various structure functions obtained without the Landau approximation.

1. Angular structure functions for electrons and photons in the approximation B

The structure functions are expanded as follows;

$$\pi_1(E_0, E, \theta, t) = \pi_1^{(0)} + \frac{1}{\Omega}\pi_1^{(1)} + \cdots \ , \tag{4·28}$$

$$\gamma_1(E_0, W, \theta, t) = \gamma_1^{(1)} + \frac{1}{\Omega}\gamma_1^{(1)} + \cdots \ , \tag{4·29}$$

$$\Pi_1(E_0, 0, \theta, t) = \Pi_1^{(0)} + \frac{1}{\Omega}\Pi_1^{(1)} + \cdots \ , \tag{4·30}$$

where π_1 and γ_1 are the angular structure functions of electrons and photons with energy $(E, E+dE)$ and $(W, W+dW)$ respectively as defined in §3.

These structure functions are given by;

$$\pi_1^{(0)} = -\frac{1}{8\pi^4 i}\int\!\!\!\int\!\!\!\int_{-i\infty}^{+i\infty} dsdpdq\Big(\frac{E_0}{E}\Big)^s \frac{1}{E}\Big(\frac{E}{K}\Big)^2\Big(\frac{\varepsilon}{E}\Big)^q\Big(\frac{E^2\theta^2}{K^2}\Big)^{-p-1}$$

$$\times \Gamma(p+1)\Gamma(-q)\mathfrak{M}_1(p, 0, q, s, t), \tag{4·28'}$$

$$\gamma_1^{(0)} = -\frac{1}{8\pi^4 i}\int\!\!\!\int\!\!\!\int_{-i\infty}^{+i\infty} dsdpdq\Big(\frac{E_0}{W}\Big)^s \frac{1}{W}\Big(\frac{W}{K}\Big)^2\Big(\frac{\varepsilon}{W}\Big)^q\Big(\frac{W^2\theta^2}{K^2}\Big)^{-p-1}$$

$$\times \Gamma(p+1)\Gamma(-q)\mathfrak{M}_1'(p, 0, q, s, t), \tag{4·29'}$$

$$\Pi_1^{(0)} = -\frac{1}{4\pi^3}\int\!\!\!\int_{-i\infty}^{+i\infty} dsdp\Big(\frac{E_0}{\varepsilon}\Big)^s\Big(\frac{\varepsilon}{K}\Big)^2\Big(\frac{\varepsilon^2\theta^2}{K^2}\Big)^{-p-1}$$

$$\times \Gamma(p+1)\Gamma(2p+s)\mathfrak{M}_1(p, 0, -s-2p, s, t), \tag{4·30'}$$

and

$$\pi_1^{(1)} = \frac{1}{8\pi^4 i}\int\!\!\!\int\!\!\!\int_{-i\infty}^{+i\infty} dsdpdq\Big(\frac{E_0}{E}\Big)^s \frac{1}{E}\Big(\frac{E}{K}\Big)^2\Big(\frac{E^2\theta^2}{K^2}\Big)^{-p-2}\Big(\frac{\varepsilon}{E}\Big)^q$$

$$\times \Gamma(p+2)(p+1)\Gamma(-q)$$

$$\times \Big\{\psi(p+2) + \psi(-p-1) - \ln\Big(\frac{E^2\theta^2}{K^2}\Big)\Big\}\mathfrak{M}_1(p, 1, q, s, t), \tag{4·28''}$$

$$\gamma_1^{(1)} = \frac{1}{8\pi^4 i}\int\!\!\!\int\!\!\!\int_{-i\infty}^{+i\infty} dsdpdq\Big(\frac{E_0}{W}\Big)^s \frac{1}{W}\Big(\frac{W}{K}\Big)^2\Big(\frac{W^2\theta^2}{K^2}\Big)^{-p-2}\Big(\frac{\varepsilon}{W}\Big)^q$$

$$\times \Gamma(p+2)(p+1)\Gamma(-q)$$

$$\times \Big\{\psi(p+2) + \psi(-p-1) - \ln\Big(\frac{W^2\theta^2}{K^2}\Big) + \frac{\partial}{\partial p}\ln{}'C(s+2p+2+q)\Big\}$$

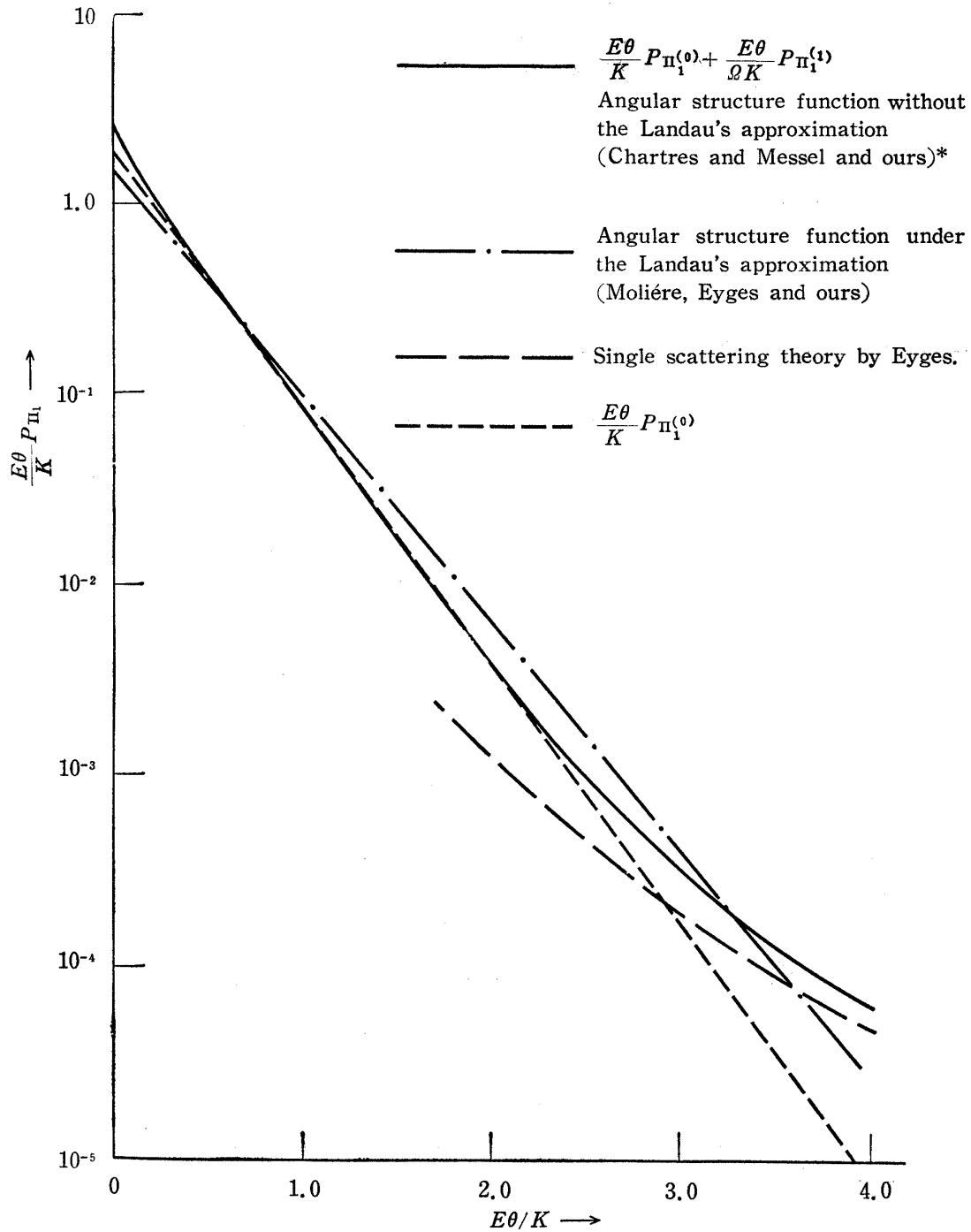$$\times \mathfrak{M}_1'(p, 1, q, s, t), \tag{4·29''}$$

Fig. 6. Normarized differential angular structure function, P_{π_1} ($s=1$), in the air in the approximation A.

P_{π_1} is normarized as

$$\int_0^\infty 2\pi \frac{E\theta}{K} d\frac{E\theta}{K} P_{\pi_1} = 1$$

with $K=19.3$ MeV and $\Omega=15.3$.

* The difference between Chartres's curve and ours is so small that it can not be represented in this figure.

$$
\Pi_1^{(1)} = \frac{1}{4\pi^3} \int\limits_{-i\infty}^{+i\infty}\!\!\int ds dp \left(\frac{E_0}{\varepsilon}\right)^s \left(\frac{\varepsilon}{K}\right)^2 \left(\frac{\varepsilon^2\theta^2}{K^2}\right)^{-p-2}
$$

$$
\times \Gamma(p+2)\Gamma(2p+2+s)(p+1)
$$

$$
\times \left[\left\{\psi(p+2) + \psi(-p-1) - \ln\left(\frac{\varepsilon^2\theta^2}{K^2}\right) + 2\psi(2p+s+2)\right\}\right.
$$

$$
\left.\times \mathfrak{M}_1(p,1,-2p-s-2,s,t) - 2\frac{\partial}{\partial q}\mathfrak{M}_1(p,1,q,s,t)\Big|_{q=-2p-s-2}\right], \quad (4\cdot30'')
$$

where $\mathfrak{M}_1$ and $\mathfrak{M}_1'$ are defined by

$$
\sum_{n=0}^{p}{}_pC_n\left(-\frac{1}{\Omega}\right)^n L^{(n)}(s+2p+2u+q)\mathfrak{M}_1(p-n,n+u,q,s,t)
$$

$$
= p\mathfrak{M}_1(p-1,u,q,s,t) + u\mathfrak{M}_1(p,u-1,q,s,t) + (s+2p+2u+q)
$$

$$
\times q\mathfrak{M}_1(p,u,q-1,s,t) - \frac{2}{\Omega}pq\mathfrak{M}_1(p-1,u+1,q-1,s,t), \quad (4\cdot31)
$$

and

$$
\mathfrak{M}_1'(p,q,s,t) = \int_0^t C(s+2p+2u+q)e^{-\sigma_0(t-t')}\mathfrak{M}_1(p,q,s,t)dt' \quad (4\cdot32)
$$

with following boundary conditions.

For the shower from a primary electron

$$
\mathfrak{M}_1(0,0,0,s,t) = H_1(s)e^{\lambda_1(s)t} + H_2(s)e^{\lambda_2(s)t}, \quad (4\cdot33)
$$

and for the shower from a primary photon,

$$
\mathfrak{M}_1(0,0,0,s,t) = \frac{B(s)}{\lambda_1(s)-\lambda_2(s)}\{e^{\lambda_1(s)t} - e^{\lambda_2(s)t}\}. \quad (4\cdot34)
$$

2. Lateral structure functions for electrons and photons in the approximation B

The structure functions are also expanded as shown above, and are given by:

$$
\pi_2 = \pi_2^{(0)} + \frac{1}{\Omega}\pi_2^{(1)} + \cdots \quad , \quad (4\cdot35)
$$

$$
r_2 = r_2^{(0)} + \frac{1}{\Omega}r_2^{(1)} + \cdots \quad , \quad (4\cdot36)
$$

$$
\Pi_2 = \Pi_2^{(0)} + \frac{1}{\Omega}\Pi_2^{(1)} + \cdots , \quad (4\cdot37)
$$

where π_2 and r_2 are the structure functions of electrons and photons with

energy $(E, E + dE)$ and $(W, W + dW)$ respectively, and Π_2 the lateral structure functions of total electrons.

These functions are given by:

$$\pi_2^{(0)} = -\frac{1}{8\pi^4 i} \int\int\int_{-i\infty}^{+i\infty} ds\, dp\, dq \left(\frac{E_0}{E}\right)^s \frac{1}{E}\left(\frac{E}{K}\right)^2\left(\frac{\varepsilon}{E}\right)^q\left(\frac{E^2 r^2}{K^2}\right)^{-p-1}$$

$$\times \Gamma(p+1)\Gamma(-q)\mathfrak{M}_2(p, 0, q, s, t), \tag{4.35$'$}$$

$$\gamma_2^{(0)} = -\frac{1}{8\pi^4 i} \int\int\int_{-i\infty}^{+i\infty} ds\, dp\, dq \left(\frac{E_0}{W}\right)^s \frac{1}{W}\left(\frac{W}{K}\right)^2\left(\frac{\varepsilon}{W}\right)^q\left(\frac{W^2 r^2}{K^2}\right)^{-p-1}$$

$$\times \Gamma(p+1)\Gamma(-q)\mathfrak{M}_2'(p, 0, q, s, t), \tag{4.36$'$}$$

$$\Pi_2^{(0)} = -\frac{1}{4\pi^3} \int\int_{-i\infty}^{+i\infty} ds\, dp \left(\frac{E_0}{E}\right)^s\left(\frac{\varepsilon}{K}\right)^2\left(\frac{\varepsilon^2 r^2}{K^2}\right)^{-p-1}$$

$$\times \Gamma(p+1)\Gamma(2p+s)\mathfrak{M}_2(p, 0, -s-2p, s, t), \tag{4.37$'$}$$

and

$$\pi_2^{(1)} = \frac{1}{8\pi^4 i} \int\int\int_{-i\infty}^{+i\infty} ds\, dp\, dq \left(\frac{E_0}{E}\right)^s \frac{1}{E}\left(\frac{E}{K}\right)^2\left(\frac{E^2 r^2}{K^2}\right)^{-p-2}\left(\frac{\varepsilon}{E}\right)^q$$

$$\times \Gamma(p+2)(p+1)\Gamma(-q)$$

$$\times \left\{\psi(p+2) + \psi(-p-1) - \ln\left(\frac{E^2 r^2}{K^2}\right)\right\}\mathfrak{M}_2(p, 1, q, s, t), \tag{4.35$''$}$$

$$\gamma_2^{(1)} = \frac{1}{8\pi^4 i} \int\int\int_{-i\infty}^{+i\infty} ds\, dp\, dq \left(\frac{E_0}{W}\right)^s \frac{1}{W}\left(\frac{W}{K}\right)^2\left(\frac{W^2 r^2}{K^2}\right)^{-p-2}\left(\frac{\varepsilon}{W}\right)^q$$

$$\times \Gamma(p+2)(p+1)\Gamma(-q)$$

$$\times \left\{\psi(p+2) + \psi(-p-1) - \ln\left(\frac{W^2 r^2}{K^2}\right) + \frac{\partial}{\partial p}\ln\left(C(s+2p+q+2)\right)\right\}$$

$$\times \mathfrak{M}_2'(p, 1, q, s, t), \tag{4.36$''$}$$

$$\Pi_2^{(1)} = \frac{1}{4\pi^3} \int\int_{-i\infty}^{+i\infty} ds\, dp \left(\frac{E_0}{\varepsilon}\right)^s\left(\frac{\varepsilon}{K}\right)^2\left(\frac{\varepsilon^2 r^2}{K^2}\right)^{-p-2}$$

$$\times \Gamma(p+2)\Gamma(2p+s+2)(p+1)$$

$$\times \left[\left\{\psi(p+2) + \psi(-p-1) - \ln\left(\frac{\varepsilon^2 r^2}{K^2}\right) + 2\psi(2p+s+2)\right\}\right.$$

$$\left. \times \mathfrak{M}_2(p, 1, -2p-s-2, s, t) - 2\frac{\partial}{\partial q}\mathfrak{M}_2(p, 1, q, s, t)\Big|_{q=-2p-2-s}\right], \tag{4.37$''$}$$

where $\mathfrak{M}_2$ and $\mathfrak{M}_2'$ are defined by

$$\sum_{n=0}^{p} {}_pC_n\left(-\frac{1}{\Omega}\right)^n L^{(n)}(s+2p+2u+q)M(p-n,n+u,q,s,t,\xi-t)$$

$$=p(\xi-t)^2\left(1-\frac{1}{\Omega}\ln(\xi-t)^2\right)M(p-1,u,q,s,t,\xi-t)$$

$$+u(\xi-t)^2M(p,u-1,q,s,t,\xi-t)$$

$$+(s+2p+2u+q)qM(p,u,q-1,s,t,\xi-t)$$

$$-\frac{2}{\Omega}pqM(p-1,u+1,q-1,s,t,\xi-t) \tag{4·38}$$

with

$$\mathfrak{M}_2(p,u,q,s,t)=\lim_{(\xi-t)\to 0} M(p,u,q,s,t,\xi-t) \tag{4·39}$$

and

$$\mathfrak{M}_2'=\int_0^t C(s+2p+2u+q)e^{-\sigma_0(t-t')}M(p,u,q,s,t',t-t')dt' \tag{4·40}$$

with the same boundary conditions as just given by the formulae (4·33) and (4·34).

§5.   Lateral Distribution of the Energy Flow of Shower Particles

The recent advance of the experimental techniques makes it possible to observe the lateral distribution of the energy flow of extensive air showers. Several works along this line have been published[17] to date, and new information on the structure of the extensive air shower will be obtained from these experiments.

The general trend of the lateral distribution of the energy flow may be expected to be as follows:

Take an electron shower with shower age s, then the differential spectra of electrons and photons are approximately given by

$$dE/E^{s+1}, \tag{5·1}$$

where E is the energy of these particles.

Since the average distance R of the particles with energy E from the shower axis is approximately given by

$$R=K/E, \tag{5·2}$$

the energy spectrum (5·1) results in the distribution of R

$$RdR/R^{2-s}. \tag{5·3}$$

This is the lateral structure function of the shower particles.

On the other hand, the differential spectrum of the energy of these particles is

$$dE/E^s. \tag{5·4}$$

Then the lateral distribution of the energy flow of these particles is approximately given by

$$RdR/R^{3-s}. \tag{5·5}$$

This shows that the lateral distribution of energy flow is $1/R$ times steeper than that of the particle number. This is due to a simple fact that the particles with high energies are less scattered from the shower axis.

Quantitative calculation can be made as follows. Let $\Pi_E 2\pi r dr$ and $\Gamma_W 2\pi r dr$ be the lateral distributions of the energy flow of electrons and photons respectively. They are represented by the following formulae:

$$\Pi_E = \int_0^\infty dE\, E\pi_2(E_0, E, r, t), \tag{5·6}$$

$$\Gamma_W = \int_0^\infty dW\, W\gamma_2(E_0, W, r, t), \tag{5·7}$$

where π_2 and γ_2 are the lateral structure functions defined in §3.

Integration with respect to E in the formulae (5·6) and (5·7) yields,

$$\Pi_E = -\frac{\varepsilon}{4\pi^3} \int\!\!\int_{-i\infty}^{+i\infty} dsdp \left(\frac{E_0}{\varepsilon}\right)^s \left(\frac{\varepsilon}{E_s}\right)^2 \left(\frac{\varepsilon^2 r^2}{E_s^2}\right)^{-p-1}$$
$$\times \Gamma(p+1)\Gamma(s-1+2p)\mathfrak{M}_2(p, -2p-s+1, s, t), \tag{5·8}$$

$$\Gamma_W = -\frac{\varepsilon}{4\pi^3} \int\!\!\int_{-i\infty}^{+i\infty} dsdp \left(\frac{E_0}{\varepsilon}\right)^s \left(\frac{\varepsilon}{E_s}\right)^2 \left(\frac{\varepsilon^2 r^2}{E_s^2}\right)^{-p-1}$$
$$\times \Gamma(p+1)\Gamma(s-1+2p)\mathfrak{M}_2'(p, -2p-s+1, s, t). \tag{5·9}$$

It is sometimes useful to represent Π_E and Γ_W in terms of the structure function, Π_2, given in §3.

The average energy of the electrons at a distance r from the shower axis is given by $\dfrac{\Pi_E}{\Pi_2}$ and we put

$$\frac{\Pi_E}{\Pi_2} = \varepsilon\frac{r_1}{r} g_e\left(\frac{r}{r_1}\right)$$

and

$$\frac{\Gamma_W}{\Pi_2} = \varepsilon\frac{r_1}{r} g_\gamma\left(\frac{r}{r_1}\right).$$

Numerical calculations of g_e and g_γ are carried out at the shower

Table 4.

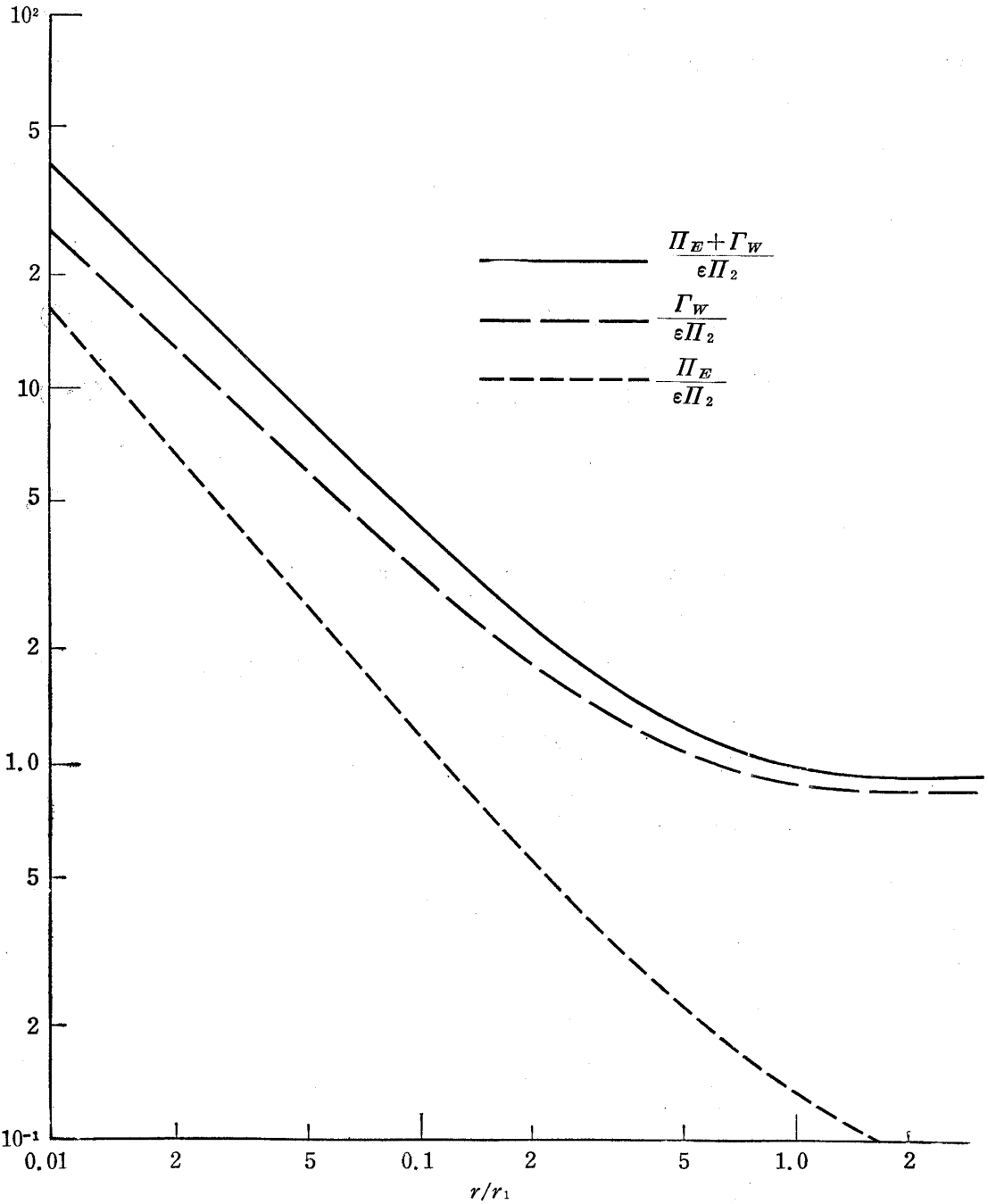| r/r_1	0	0.01	0.4	0.1	1.0	2.0	4.0
g_e (r/r_1)	0.15	0.15	0.12	0.14	0.14	0.20	0.30
g_γ (r/r_1)	0.21	0.26	0.45	0.82	0.83	1.8	3.7

Fig. 7. The relation between energy and the number of electrons at the shower maximum as a function of the distance from the shower axis.

maximum, and the results are shown in Table 4.

This shows that g is almost constant near the shower axis; thus g_e and g_γ are approximately given by $1/r^{3-s}$ as predicted in the beginning of this section.

At a large distance, however, g_e and g_γ increase nearly in proportion to the distance from the shower axis, thus the average energy of the shower particles remains almost constant in this region. The result may be interpreted in the following way. The mean free path for the pair creation of the photons remains almost constant for all over the energies. Thus low energy photons can travel up to a large distance from the shower axis, and the electrons lying in this region are produced from these low energy photons. These low energy electrons can travel only a short distance because they lose their energies by the ionization process. As a result the average energies of the shower particles at varying distances from the axis remain constant, and photons are much more accumulated at a large distance from the core compared with the electrons.

§6. Applications of Our Theory to the Cosmic Ray Phenomena

1. Application to the electron showers observed in nuclear emulsions

The recent developments in the nuclear emulsion techniques have made it possible to observe the full development of the high energy electron showers in a large stack of emulsion.

Electron showers observed in emulsion are started by a photon or an electron, or two γ rays from a π^0 meson in a jet produced in the stack. Thus the energy determination of the shower is important not only for the study of the pure electron showers but for the study of the high energy nuclear interactions.

Electron showers in emulsion are observed under a microscope usually over an area along shower axes extending to several hundred microns from the axes. For example, the K. Pinkau[18] adopted the following way. The energies of individual electrons are measured by the scattering method, and the energy spectrum of electrons within the circle of a radius r from the axis is obtained.

As shown already, high energy electrons concentrate near the core. Then, if we take the circle of a certain radius r, most of the particles with energies larger than a certain value, i. e., of the order of K/r, are lying within the circle. Thus, if we limit ourselves to such high energy electrons, they are treated by means of the linear cascade theory in the approximation A. He applied this method to several showers observed in G stacks ($12'' \times 16''$ G_5 emulsions), and could determine the energy of an incident γ ray or electron.

Another approach to the energy determination of electron showers can be made by making use of their transition curves as follows. As the radius r is at most several hundred microns, r/K is much smaller than the reciprocal critical energy. Thus, in this case, we can apply the approximation $\varepsilon r/K \ll 1$ to the expression (4·37) for the lateral structure function, and the number of electrons within a radius r is expressed as

$$\int_0^r 2\pi r dr \Pi_2 = \int_0^r 2\pi r dr \Pi_2^{(0)} + \frac{1}{\Omega} \int_0^r 2\pi r dr \Pi_2^{(1)} + \cdots, \qquad (6\cdot1)$$

where

$$\int_0^r 2\pi r dr \Pi_2^{(0)} = \frac{1}{2\pi i} \int_{-i\infty}^{+i\infty} \frac{ds}{s} \left(\frac{E_0 r}{K}\right)^s \Gamma\left(1 - \frac{s}{2}\right) \mathfrak{M}_2\left(-\frac{s}{2}, 0, 0, s, t\right)$$

and $(6\cdot2)$

$$\int_0^r 2\pi r dr \Pi_2^{(1)} = \frac{1}{4\pi i} \int_{-i\infty}^{+i\infty} ds \left(\frac{E_0 r}{K}\right)^s \Gamma\left(1 - \frac{s}{2}\right) \left[\psi\left(1 + \frac{s}{2}\right)\right.$$

$$\left. \times \mathfrak{M}_2\left(-1 - \frac{s}{2}, 1, 0, s, t\right) - \frac{\partial}{\partial p}\mathfrak{M}_2(p, 1, 0, s, t)\Big|_{p=-1-\frac{s}{2}}\right]. \qquad (6\cdot3)$$

It should be remarked that E and r in the above formulae always appear as a combined product Er/K, not as separate variables. This makes the expression very convenient for making practical applications.

The numerical calculations of the above expressions for the shower of an incident γ ray are carried out, and the results are shown in Table 5.

Table 5.

Number of electrons of a photon-iniciated-shower within a circle of radius r in emulsions calculated without the Landau approximation.

E : energy of the incident photon

t : depth in emulsions measured in cascade units.

1 C. U. = 2.83 cm in G_5 emulsions.

$Er(\text{Gev}\mu)$ $\diagdown$ t	$5 \cdot 10^3$	10^4	$2 \cdot 10^5$	$5 \cdot 10^4$	10^5	$2 \cdot 10^5$
1C. U.	1.8	2.15	2.45	2.8	3 0	3.2
2	4.0	5.7	8.5	12.1	15.1	18.1
3	5.3	8.2	12.6	20.6	29.5	41.0
4	5.7	10.2	18.2	33.7	52.0	79.0
5	4.6	9.5	19.0	39.0	67.0	110
6	2.6	6.4	14.5	34.0	66.0	125
8	1.0	3.0	8.5	25.0	55.0	120

The table displays the behavior of the transition of the number of electrons

within a radius r, and therefore gives the lateral distribution of electrons under a certain cascade unit.

Comparing the observed transition curves with our theoretical curves, we can determine the energy of the electron showers without making any
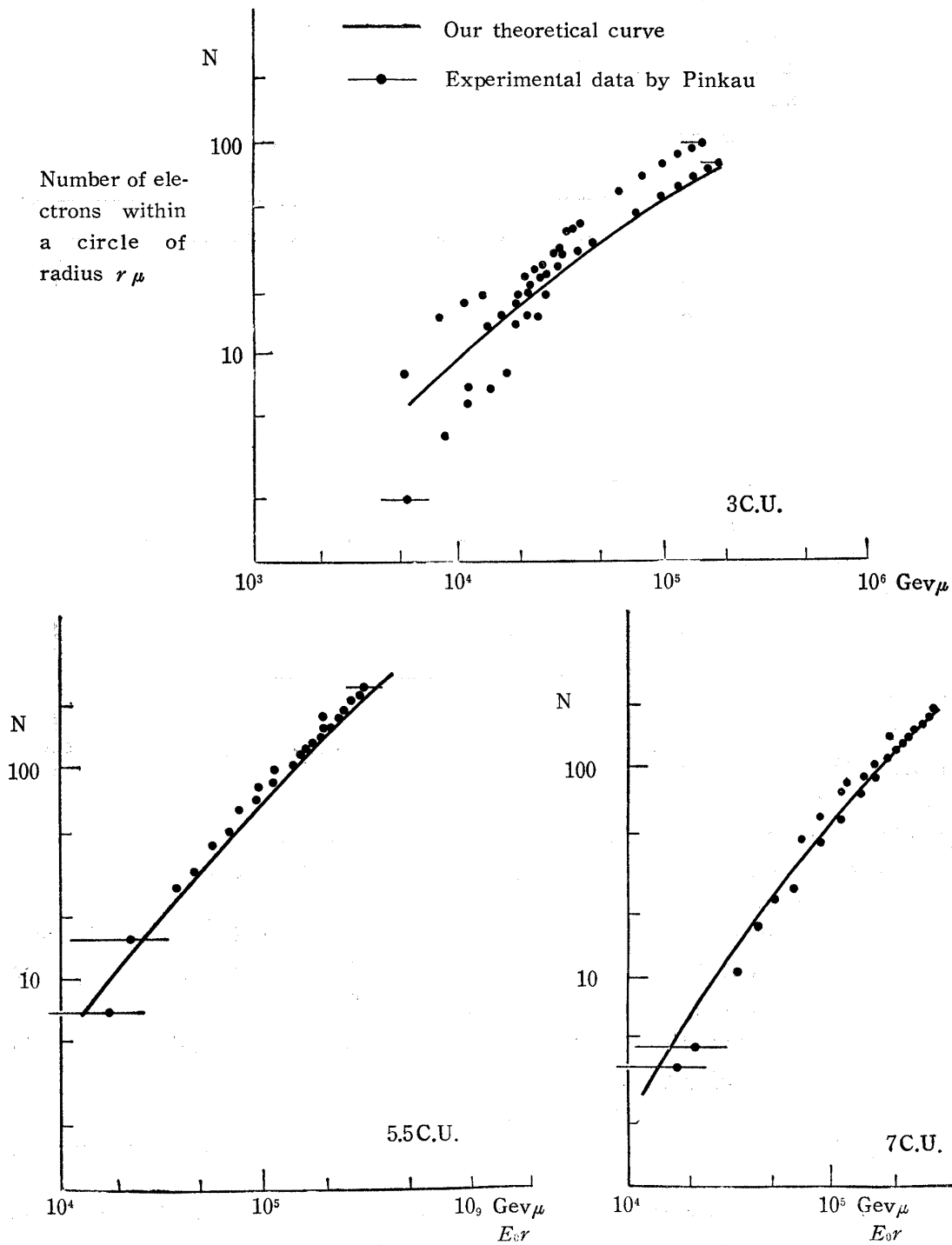

Fig. 8.   Comparison of our theoretical curves with Pinkau's data. Depth quated here is measured from the point of incident pair electrons.

tedious scattering measurement of the particles.

In Fig. 8, comparison is made between Pinkau's data and the theoretical curves, and the agreement is fairly good.

An extensive application of our theory to the electron showers in emulsion was made in the so-called "Emulsion Chamber project"[19] which was carried out through collaboration of several laboratories in Japan. The project was made to study the dynamical properties of high energy jet showers in cosmic rays.

The illustration of the chamber is in Fig. 9, in which the material of the low atomic number is put in the upper half of the chamber as the producing layers of the jet showers, and the high Z material below as the detection layers of the electron showers from a produced π° meson.

If a jet shower is produced in the upper half of the chamber, the γ rays from π° mesons generate the electron showers in the detection layers after penetrating through the low Z material

Type A.

|←———————— 20 cm ————————→|

Carbon — 10 cm

Empty Space — 4 cm

Lead — 6 cm

Fig. 9.   Illustration of the emulsion chamber.

layers without any materialization. Then, we can observe separately individual electron showers which have started from individual γ rays resulting from mesons, because the spatial separation among these γ rays becomes large by traversing a certain distance from the production point of the jet to the detection layers.

The energies of γ rays are measured by comparing our theory with the observed transition curves of the number of electrons within a circle of radius r under the successive lead plates, an example of which is shown in Fig. 10.

Once we observed the electron showers with a distinct double core structure, and if it is clear that they are due to two γ rays from a π° meson, then we can make an independent test of the precision of our theories.
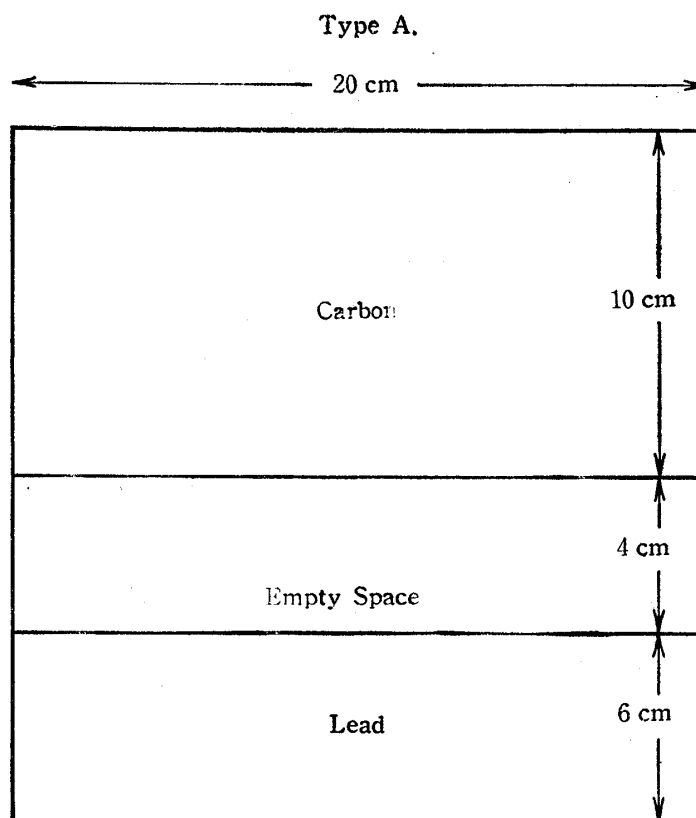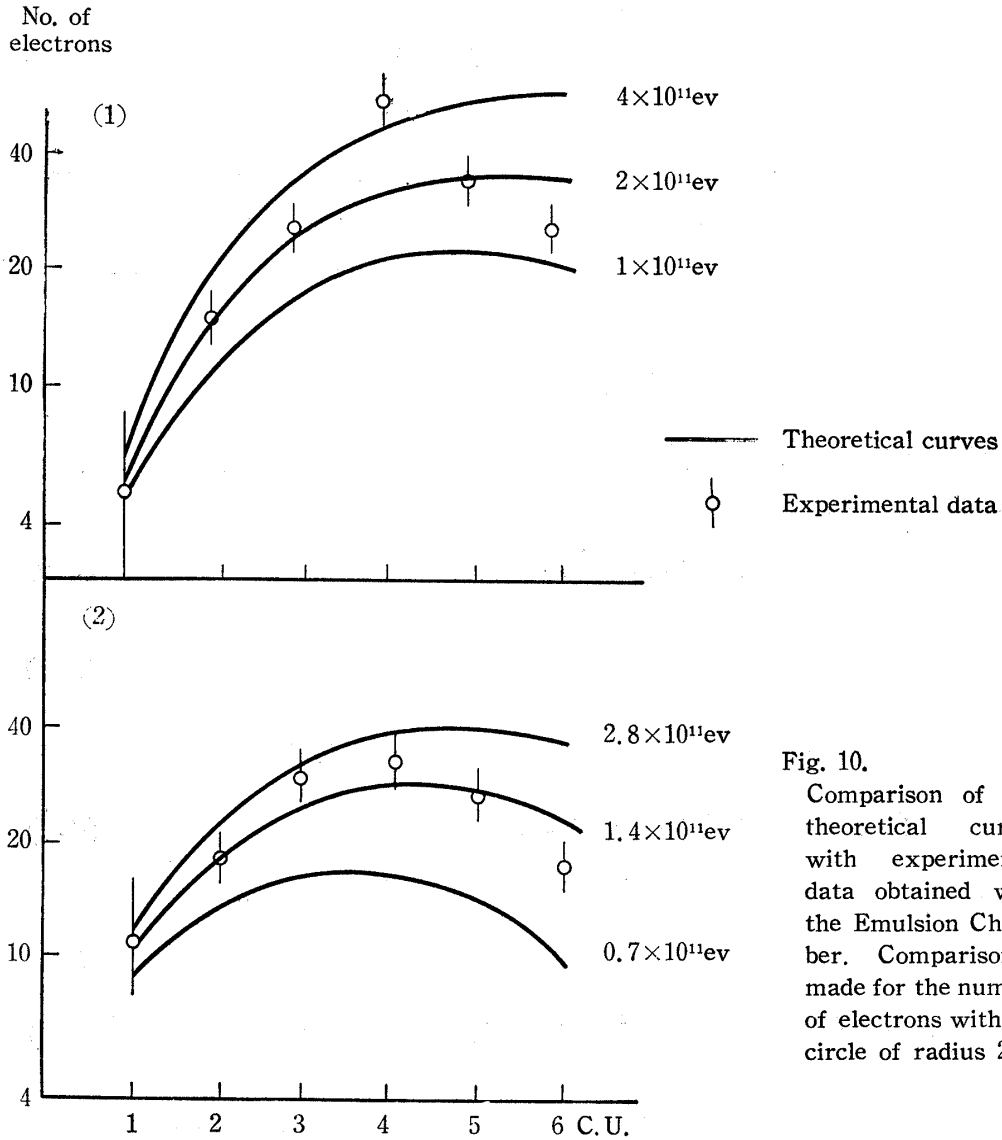
No. of
electrons

Fig. 10.
Comparison of our theoretical curves with experimental data obtained with the Emulsion Chamber. Comparison is made for the number of electrons within a circle of radius 25μ.

Using the kinematical relation between the opening angle of the two γ rays from a π° meson and its energy, we can get information on the energies of these γ rays. The energies thus determined are compared with those estimated from their cascade transition curves, and, as shown in reference 19, the agreement is quite good.

2. Application of our Theory to the Extensive Air Showers

As is known, electron showers observed in an extensive air shower start from many π° mesons which are produced at each step of a nucleon cascade in the atmosphere. Thus our structure function should not be compared directly with that observed in extensive air showers.

The electron showers having many sources distributed in space can be

treated in the following way.

First we consider a simple case in which π° mesons are produced only in the shower axis and decayed γ rays run in the same direction as the axis of the air showers.

Let $F(E_0, t)\,dE_0dt$ be the number of such γ rays with energy $(E_0, E_0 + dE_0)$ that decayed from the π° mesons produced at the depth between t and $t+dt$ cascade units below the top of the atmosphere. Then the structure function Π at the depth T is given by

$$\Pi = \int_0^\infty dE_0 \int_0^T dt\, F(E_0, t)\Pi_2(E_0, 0, r, T-t). \tag{6·4}$$

Substituting the formula (3·28) in (6·4), and integrating with respect to E_0 and t, we get

$$\Pi \sim L_F(s, T)f(r, s)e^{\lambda_1(s)T}, \tag{6·5}$$

where

$$L_F(s, t) = \int_0^\infty dE_0(E_0/\varepsilon)^s \int_0^T dt\, F(E_0, t)e^{-\lambda_1(s)t}, \tag{6·6}$$

and $f(r, s)$ is the structure function of shower age s, s being defined by

$$(1/L_F)\frac{dL_F(s)}{ds} + \lambda_1(s)T = 0. \tag{6·7}$$

The absorption mean free path of these particles, L, at the depth T can be derived from the equation (6·5), and it is given, using (6·5), by

$$-(1/L) = (1/L_F)\frac{dL_F}{dT} + \lambda_1(s). \tag{6·8}$$

As L_F is a monotonously increasing function of T, we get from (6·8)

$$1/L \geq \lambda_1(s). \tag{6·9}$$

Taking 150—250 gr/cm² of air as the observed valuse of L at mountain altitudes,

$$\lambda_1(s) \leq -0.15 \sim -0.25.$$

Then we have

$$s \geq 1.2 \sim 1.4.$$

Now, it becomes evident that the structure function in this case can be represented by that of a single cascade with shower age s, which is determined with the aid of the absorption mean free path L at such a large distance from the axis that the spread of the parent particles can be neglected.
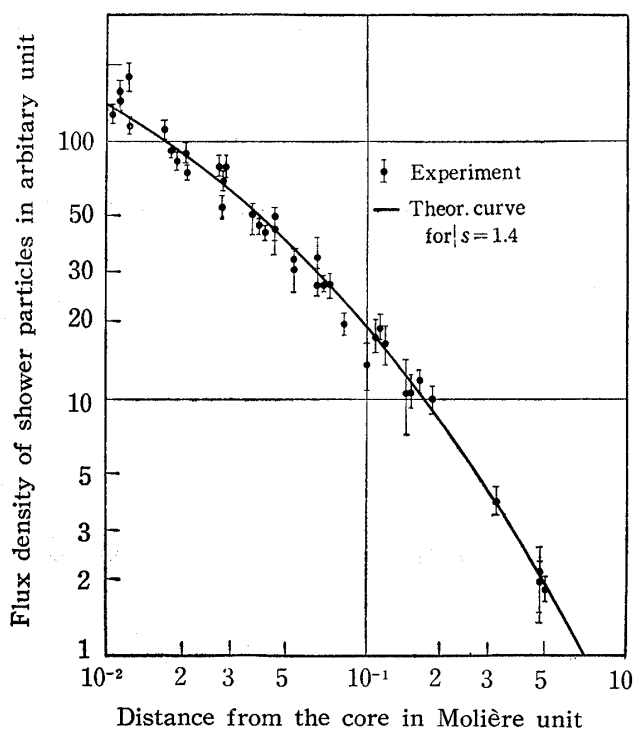
Fig. 11. Comparison of Structure Function with Experiment. Experimental results were obtained at Pamir Mountain (3860) by Soviet group, and the solid line represents the structure function for $s=1.4$.

At the center of air showers, the spread of main sources can no longer be neglected. The observed structure function deviates from that of the single cascade, and from this deviation the magnitude of the spread of main sources can be estimated.

Comparison of the one observed by Soviet group[20] with ours is made in Fig. 11, and this deviation appears within a few meters from the shower axis.

Mathematical treatment including the source spread can also be made by using the Bessel transforms, assuming the shape of this spread.

From the spread of these main sources, we get information on the transverse momenta of high energy π° mesons, the values of which are estimated to be ranging from 100 Mev/c to 1000 Mev/c for π° mesons with energies $10^{12}-10^{13}$ ev.

Along the line of such considerations one of us (J. N) has pointed out the importance of the properties of the transverse momentum by referring to the data obtained with emulsion.

§7. Discussion and Summary

Three dimensional cascade theories here presented are based on the approximation B with and without the Landau approximation. Thus the theories are developed with fewer physical assumptions than any other theory. It is pointed out that the structure functions of the number and the energy density of the shower particles near the shower axis are well approximated by $1/r^{2-s}$ and $1/r^{3-s}$, where s is the shower age of the cascade.

The theories are applied successfully to the analysis of the lateral spread of the extensive air showers and the electron showers observed in large stacks of emulsion.

It seems worthwhile to examine the relation between our theories and several other theories.

1) Molière's theory[3]

The Molière function was the first one that has been extensively used for the analysis of the structure of extensive air showers. In his theory, Molière started from the Landau equation in the approximation A. After the Fourier transformation of this equation, the solution at $s=1$ was obtained in a form of power series of x^{2n}. The series are just the same as our solution (3·10) at $s=1$ in section 3.

He approximated this series by

$$\frac{a}{(1+\alpha^2 x^2)^{3/2}} - \frac{a-1}{(1+\beta^2 x^2)^{5/2}} , \tag{7·1}$$

where a, α, and β are constants and are given by

$$a = 3.473$$
$$\alpha = 1.05$$
$$\beta = 0.912 .$$

Applying the inverse Fourier transformation to the above, he got the lateral distribution in the approximation A at shower maximum $(s=1)$. The contribution of the low energy particles was taken into account by using Arley's approximation. As is well known, the number of particles with energies smaller than the critical energy is evaluated to be too small in this approximation than in the exact theory. Thus, his theory would give us the steeper lateral structure function, because the contribution of the scattering is inversely proportional to the energy of the particles.

In spite of the above differences between the approximations made in the two theories, his function agrees quite well with ours at $s=1$ as shown in Fig. 3.

2) Roberg and Nordheim's theory[5]

In their ingenious treatment, referring to the one dimensional cascade theory, they have derived the expressions of $\langle r^{2n} \rangle_{av.}$ and $\langle \theta^{2n} \rangle_{av.}$ in integral forms.

The equivalence between their theory and ours, can be proved as follows:
As shown in §3, $\langle r^{2n} \rangle_{av.}$ and $\langle \theta^{2n} \rangle_{av.}$ in our theory are represented by;

$$\langle r^{2n}\rangle_{av.} = \frac{\int_0^\infty r^{2n}\pi_2 2\pi r\,dr}{\int_0^\infty \pi_2 2\pi r\,dr} = \frac{n!\,E_s^{2n}}{E^{2n}}\cdot\frac{\mathfrak{M}_2(p=n,\,q=0,\,s,\,t)}{\mathfrak{M}_2(p=0,\,q=0,\,s,\,t)}\,, \qquad (7\cdot 2)$$

$$\langle \theta^{2n}\rangle_{av.} = \frac{\int_0^\infty \theta^{2n}\pi_1 2\pi\theta\,d\theta}{\int_0^\infty \pi_1 2\pi\theta\,d\theta} = \frac{n!\,E_s^{2n}}{E^{2n}}\cdot\frac{\mathfrak{M}_1(p=n,\,q=0,\,s,\,t)}{\mathfrak{M}_1(p=0,\,q=0,\,s,\,t)}\,. \qquad (7\cdot 3)$$

Since

$$\mathfrak{M}_1(p=n,\ q=0,\,s,\,t)$$

$$= n\int_0^t \mathfrak{M}_1(p=n-1,\ q=0,\,s,\,t')\mathfrak{M}_1(p=0,\,q=0,\,s+2n,\,t-t')dt',$$

$$(7\cdot 4)$$

and

$$\mathfrak{M}_2(p=n,\ q=0,\,s,\,t)$$

$$= n\int_0^t \mathfrak{M}_2(0,0,\,s+2n,\,t-t')(t-t')^2 M(n-1,0,\,s,\,t',\,t-t')dt',$$

they give

$$(7\cdot 5)$$

$$\langle r^{2n}\rangle_{av.} = n!\,n\left(\frac{E_s}{E}\right)^{2n}\frac{\int_0^t \mathfrak{M}_2(0,0,s+2n,t-t')(t-t')^2 M(n-1,0,s,t',t-t')dt'}{\mathfrak{M}_2(0,0,s,t)}\,,$$

and

$$(7\cdot 6)$$

$$\langle \theta^{2n}\rangle_{av.} = n!\,n\left(\frac{E_s}{E}\right)^{2n}\frac{\int_0^t \mathfrak{M}_1(0,0,s+2n,t-t')\mathfrak{M}_1(n-1,0,s,t')dt'}{\mathfrak{M}_1(0,0,s,t)}\,.$$

$$(7\cdot 7)$$

These expressions are just the same formulae as those given by Roberg and Nordheim.

For the numerical calculation they have used cross sections for the radiation and the pair creation somewhat different from ours. The results of their numerical evaluation in comparison with ours are shown in Table 6 and the agreement between these two is fairly good.

3) Eyges and Fernbach's theory[1]

At first, they have derived the recurrence formulae of $\langle r^{2n}\rangle_{av.}$ and $\langle \theta^{2n}\rangle_{av.}$ from the Laundau equation in the approximation A. The structure functions were constructed using the moments which were derived from the above recurrence fomulae. Afterward, the contribution of the ionization loss is also taken into account in an approximate way.

As $\mathfrak{M}_2(p)$ and $\mathfrak{M}_1(p)$ have close connection with $\langle r^{2n}\rangle_{av.}$ and $\langle \theta^{2n}\rangle_{av.}$

Table 6. Mean square average of the structure function for $s=1.0$. The comparison of Roberg-Nordheim's results (abbreviated as R-N in Table 6) with ours. Here,

$$\langle r^2\rangle_{av.}=\frac{\int_0^\infty r^2\pi_2 2\pi r\,dr}{\int_0^\infty \pi_2 2\pi r\,dr} \quad \text{and} \quad \langle r_T^2\rangle_{av.}=\frac{\int_E^\infty dE\int_0^\infty r^2\pi_2 2\pi r\,dr}{\int_E^\infty dE\int_0^\infty \pi_2 2\pi r\,dr}.$$

E/ε	$\langle r^2\rangle_{av.}$		$\langle r_T^2\rangle_{av.}$	
	R–N	Ours	R–N	Ours
∞	$0.642\left(\dfrac{E_s}{E}\right)^2$	$0.723\left(\dfrac{E_s}{E}\right)^2$	$0.214\left(\dfrac{E_s}{E}\right)^2$	$0.241\left(\dfrac{E_s}{E}\right)^2$
10	0.49	0.58	0.18	0.20
7	0.46	0.53	0.17	0.18
5	0.43	0.46	0.16	0.17
3	0.40	0.36	0.14	0.14
2	0.33	0.28	0.125	0.11
1.5	0.30	0.22	0.105	0.090
1.0	$0.25\left(\dfrac{E_s}{\varepsilon}\right)^2$	$0.15\left(\dfrac{E_s}{\varepsilon}\right)^2$	$0.085\left(\dfrac{E_s}{\varepsilon}\right)^2$	$0.064\left(\dfrac{E_s}{\varepsilon}\right)^2$
0.75	0.28	0.21	0.12	0.087
0.5	0.39	0.32	0.165	0.125
0.4	0.46	0.40	0.19	0.16
0.3	0.60	0.53	0.235	0.19
0.2	0.86	0.82	0.31	0.26
0.15	1.13	1.02	0.48	0.31
0.10	1.6	1.31	0.46	0.39
0.05	2.8	1.58	0.64	0.53

and as our difference equations for $\mathfrak{M}(p)$ with positive integer p have just the same forms with their recursion equation, it may easily be seen that their treatment is included in our theory as a special case of our theory.

4) Messel and Green's theory[21]

They have pointed out the importance of the higher moments of scattering angles in the Rutherford cross section. Then, they set up the equation including $(K_0^2\zeta^2/4E^2)+(K_1^2\zeta^2/4E^2)^2+\cdots$, instead of using $(E_s^2\zeta^2/4E^2)$ in equation (3·5).

In their general approach, they have also calculated in the approximation A the second moments of the structure function of the cascade developed in the isothermal atmosphere.

In our theory, the higher moments of the Rutherford scattering angles are taken into account in the structure function derived without the Landau

approximation.

The second moment of their structure function in the isothermal air just coincides with ours as shown in appendix II.

5) Green and Bergmann's theory[22]

The behavior of the differential structure function near the core of Molière's as well as of ours is represented by

$$r^{-2+s+(2/3)}$$

in the approximation A. On the other hand, in their treatment without the Landau approximation, Green and Bergmann proved that the singularity is expressed more exactly by

$$A\left(\frac{\delta(r)}{r} + B\frac{1}{r} + C\ln r\right),$$

where A, B, and C are the function of t.

They have also stated that the different behaviors presented by other theories are due to the different approximations used by respective authors and, consequently, that Molière's function and ours give incorrect behaviors near the core.

It can be proved, however, that the singularity remains to be the same as in formula (3·43), even if we take the structure function without the Landau approximation derived in §4. The behavior near the core is mainly determined by the following two reasons.

(1) At the first stage of the development of the cascade showers, the thickness of the traversed matter is thin enough, so that the particles are scarcely scattered. Then the particles remain near the core without suffering the scattering.

(2) The ancestors with higher energies, which are less scattered from the core, produce more particles. As a result particles accumulate near the core.

It can be shown that the singularity presented by Green and Bergmann is in fact due to the former reason, (1), while ours is due to the latter, (2).

Since the cross section of the Rutherford scattering is so large that the probability without suffering any scattering is much reduced after traversing the proper thickness of material. Thus the singularity due to the reason (1) is practically less important in an actual case, even if the order of singularity of the structure function due to (1) is higher than that which is due to the reason (2).

In fact, for the showers under the proper thickness, say twenty cascade units or so, it can be proved that the absolute value of our structure func-

tion is much larger than that obtained by themselves for $r > 10^{-5}$ mm in the air at a mountain altitude.

In conclusion, the authors express their appreciation to Prof. Y. Fujimoto and Prof. S. Hayakawa for their stimulating discussions throughout this work, and to Prof. J. M. Blatt, Prof. K. Greisen and Prof. H. Messel for their kind and valuable comments on this work. The authors are also indebted to the members of the air shower group in Japan for their helpful discussions, and Mrs. H. Aizu and Mr. A. Tachibana for their numerical culculations.

Appendices

I. Approximate Formulae for our structure functions.

Since the evaluation of our structure functions requires the long and tedious numerical calculations as stated in Appendix IV, it will be very convenient to set up a simple asymptotic formula for the practical applications.

The following formula, $f(r/r_1, s)$ was derived from the numerical results of $P_{\text{II}_2}(r/r_1, s)$ illustrated in Figs. 2, 3, 4, and 5;

$$f(r/r_1, s) = \frac{c(s)}{(r/r_1)^{2-s}}\left[1 + (4/s)(r/r_1)\right]e^{-a(s)(r/r_1)^{b(s)}}, \tag{I·1}$$

which is normalized as

$$\int_0^\infty f(r/r_1, s)\, 2\pi(r/r_1)\, d(r/r_1) = 1, \tag{I·2}$$

where

$$a(s) = \frac{4}{s}e^{0.915(s-1)}, \tag{I·3}$$

$$b(s) = 0.15 + \frac{1}{1+s}, \tag{I·4}$$

$$c(s) = \frac{a^{s/b}}{2\pi\left\{\Gamma\left(\dfrac{s}{b}\right) + \dfrac{4\Gamma\left(\dfrac{s+1}{b}\right)}{sa^{1/b}}\right\}}. \tag{I·5}$$

The numerical values of $a(s)$, $b(s)$ and $c(s)$ are tabulated in Table 7.

Table 7

s	0.2	0.4	0.6	0.8	1.0	1.2	1.4	1.6	1.8	2.0
$a(s)$	9.6	5.76	4.61	4.16	4.00	4.00	4.12	4.32	4.62	5.00
$b(s)$	0.984	0.864	0.775	0.706	0.605	0.650	0.566	0.535	0.507	0.483
$c(s)$	0.042	0.101	0.189	0.306	0.462	0.64	0.87	1.20	1.68	2.30

The values $c(s)$ for the large s listed in Table 7 are somewhat different from the values given in the fromula (I·5), because the formula (I·1) does not accurately represent the structure function for $r/r_1 \gg 1$, which gives a considerable contribution to the integral (I·2) for the large s.

The formula for $s = 1.0$ shows a quite good agreement with Bethe's approximation formula derived from the Molière function which is given by,

$$f(r/r_1) = 0.45 \frac{1}{r/r_1} \left(1 + 4 \frac{r}{r_1}\right) e^{-4(r/r_1)^{2/3}} \qquad \text{(I·6)}$$
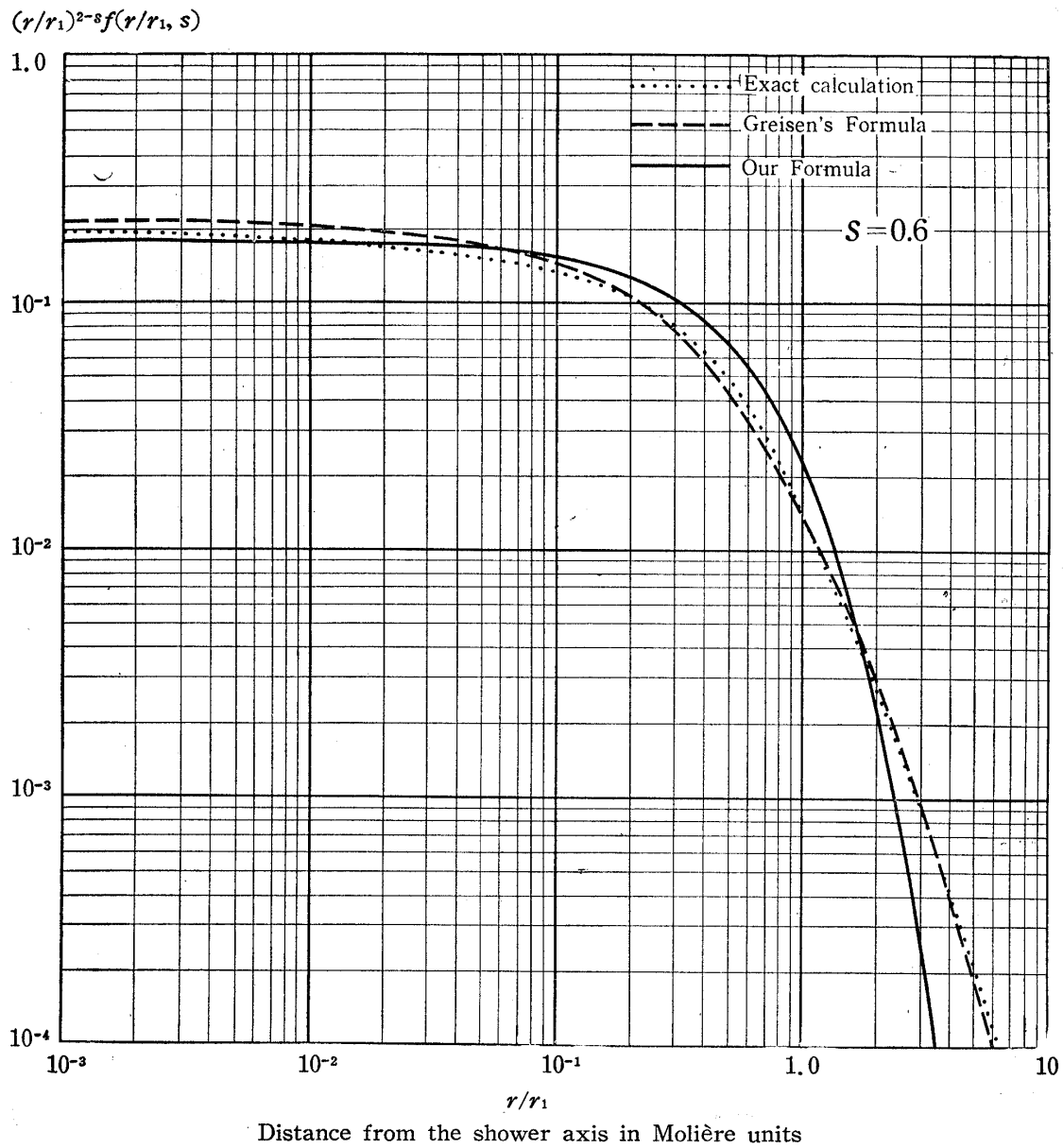
Fig. 12. Asymptotic Formula of the Structure Function for $s = 0.6$. Dotted line represents the exact calculation, dashed line Greisen's formula, and solid line our formula.

It should be noted that the formula is not applicable in the case in which the primary energy is not infinitely large when compared with the mean energy of shower particles and the details will be disccussed in Appendix III.

Recently the following formula has been proposed by Greisen,[23]

$$f(r/r_1) = c(s)(r/r_1)^{s-2}\left(1 + \frac{r}{r_1}\right)^{s-4.5},\qquad\text{(I·7)}$$

where $c(s)$ is the normalization factor. His formula is simpler than ours, but our formula (I·1) has a wider applicability than his formula.

$(r/r_1)^{2-s} f(r/r_1, s)$

Distance from the shower axis in Molière units
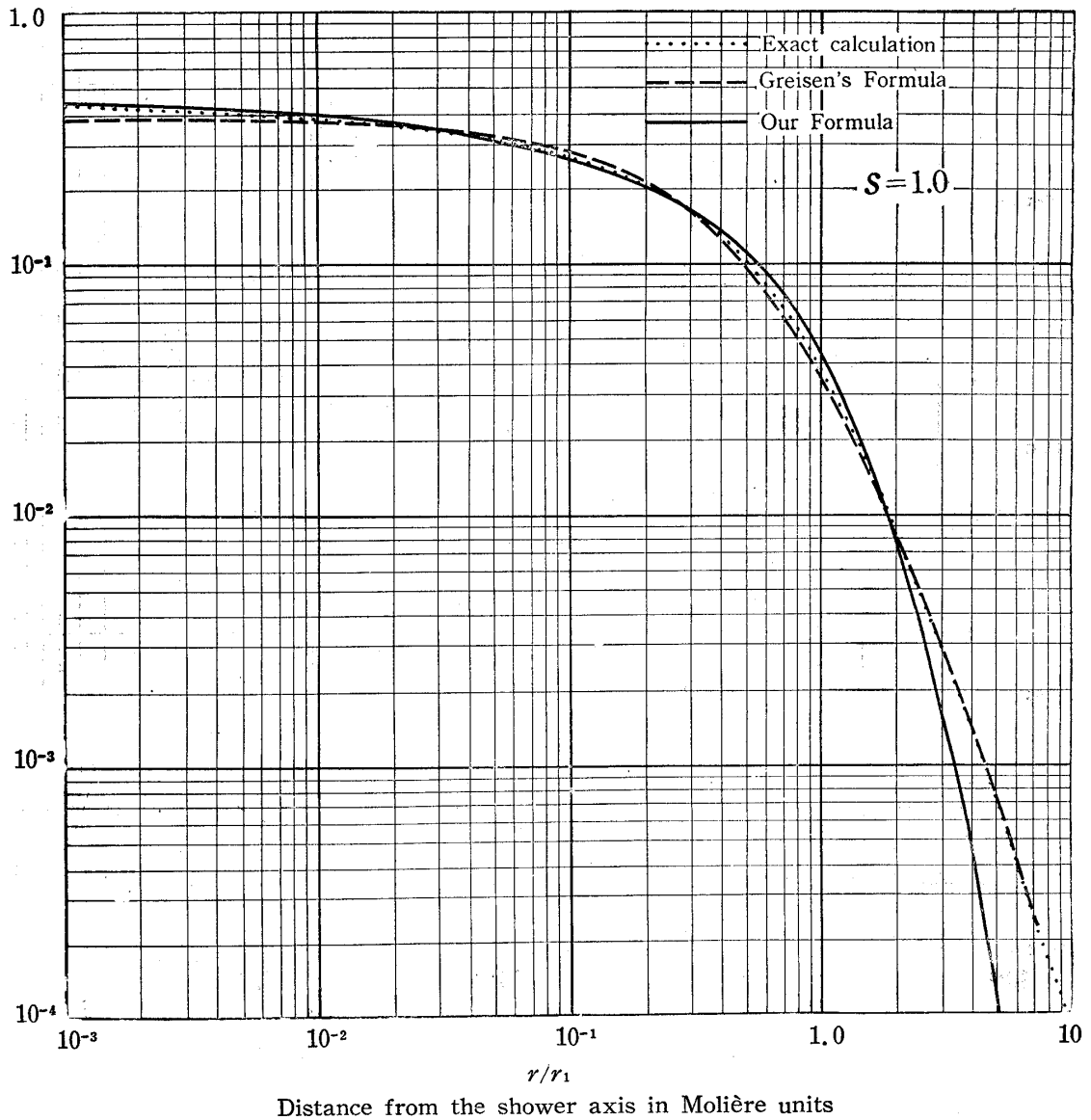
Fig. 13. Asympotic Formula of the Structure Function for $s=1, 0$,

The numerical results of our asymptotic formula are illustrated in Figs. 12, 13, 14 and 15 comparing with Greisen's formula. His formula agrees well with our formula for $0.6 < s < 1.0$ but deviates from ours for $1.4 < s \leq 2.0$.

II. Effect of the variation of the air density on the structure functions.

So far we have been limited to the calculation of the structure function only in the homogenious matter. In actual cases, however, the extensive air showers develop in the atmosphere; hence variations in the density of air with height should be taken into account in the calculation.

It is plausible to consider that the observed shower particles are mainly

$(r/r_1)^{2-s} f(r/r_1, s)$
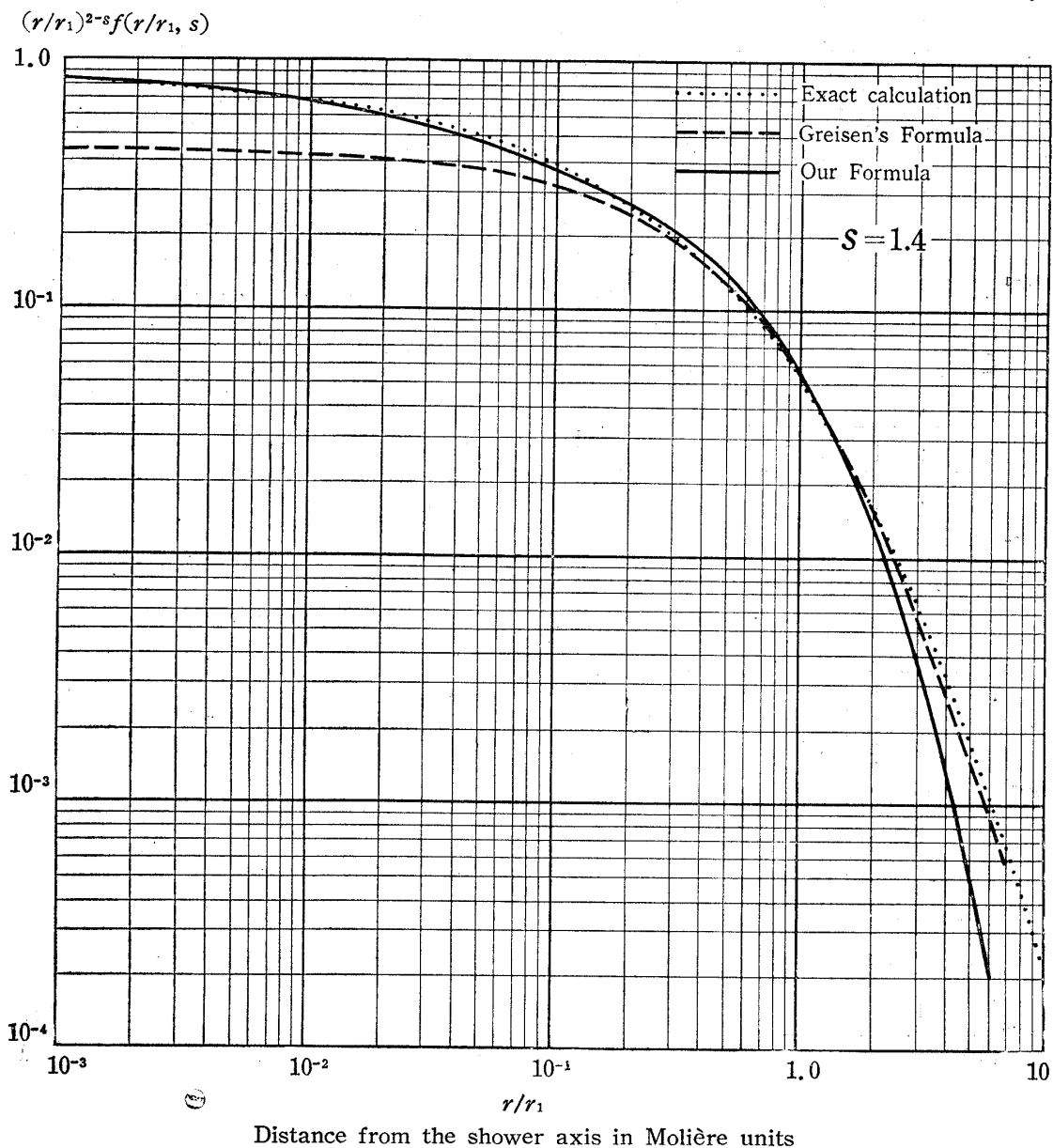
Fig. 14. Asymptotio Foimula of the Structure Function for $s=1.4$.

deflected in air between the observation point and the point that lies one
cascade unit above that in the space, because the ancesters of these particles
have much higher energies at higher altitudes, and they are less scattered

$(r/r_1)^{2-s} f(r/r_1, s)$
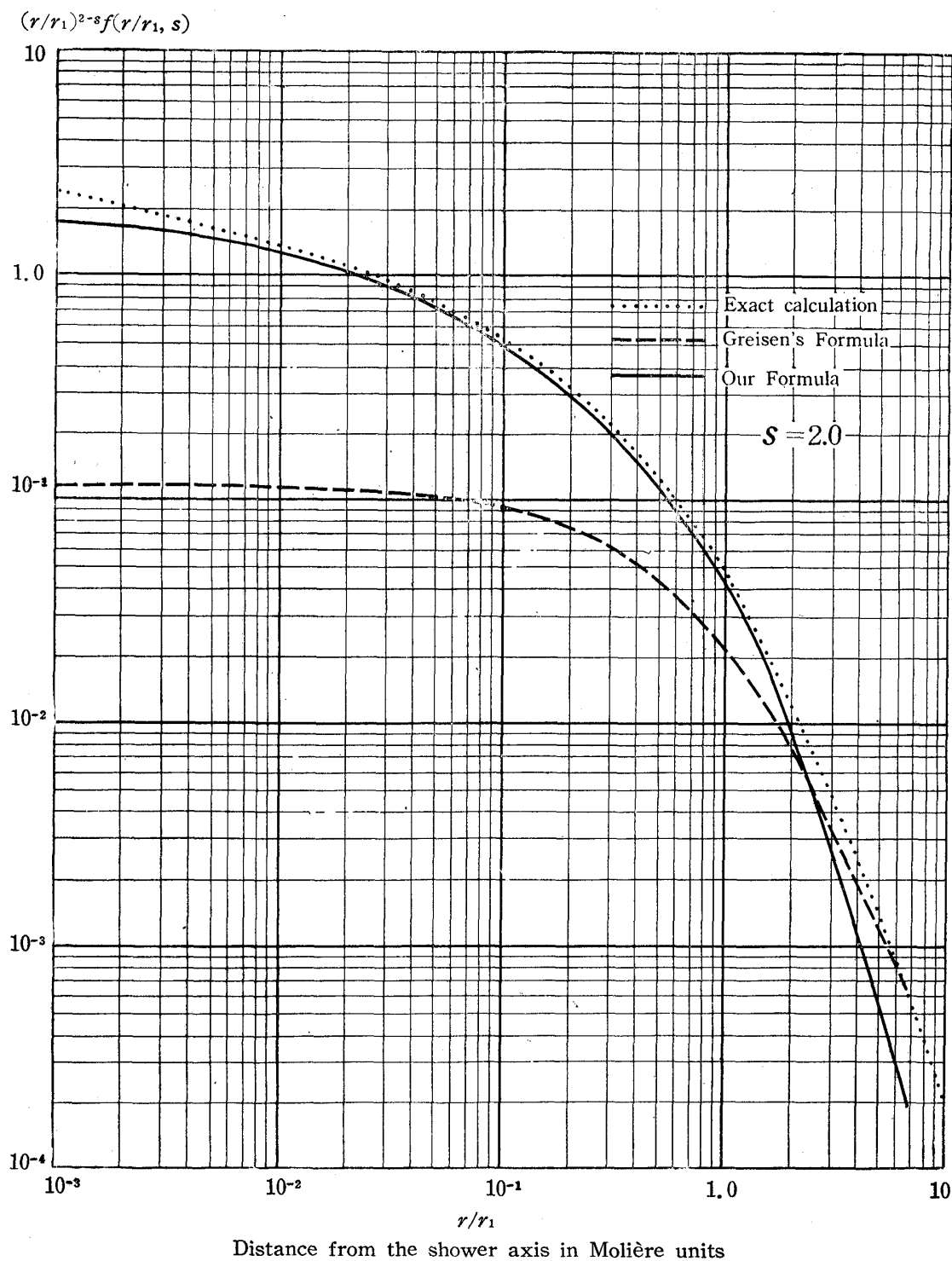

Distance from the shower axis in Molière units

Fig. 15. Asymptotic Formula of the Structure Function for $s=2.0$.

compared with the observed particles. This consideration led Janossy to point out that, if we are to make comparison between experimental data and the structure function calculated in homogeneous matter, we should take the air density at a point of one cascade unit above the observation point.

Messel and Green[21] have treated this problem in a quantitative way, but they were limited to the structure function in the approximation A.

Here we formulate the equations for the structure function in inhomogeneous matter. The Landau equations in homogeneous matter are given by equations (3·1) and (3·2), which are replaced, in inhomogeneous matter, by

$$\left[\frac{\partial}{\partial t} + \frac{\rho(T)}{\rho(t)}\left(\boldsymbol{\theta}\frac{\partial}{\partial \boldsymbol{r}}\right)\right]\pi = -A'\pi + B'\gamma + \frac{E_s}{4E^2}\nabla_\theta\pi + \varepsilon\frac{\partial\pi}{\partial E}, \qquad (\text{II}\cdot1)$$

$$\left[\frac{\partial}{\partial t} + \frac{\rho(T)}{\rho(t)}\left(\boldsymbol{\theta}\frac{\partial}{\partial \boldsymbol{r}}\right)\right]\gamma = C'\pi - \sigma_0\gamma. \qquad (\text{II}\cdot2)$$

In these equations $\rho(T)$ and $\rho(t)$ are the density at the depth T and t cascade units respectively: T is the depth of the observation point and r is measured by the length of the cascade unit at T.

The operator $\dfrac{\partial}{\partial t} + \left(\boldsymbol{\theta}\dfrac{\partial}{\partial \boldsymbol{r}}\right)$ for homogeneous matter is now replaced by

$$\frac{\partial}{\partial t} + \frac{\rho(T)}{\rho(t)}\left(\boldsymbol{\theta}\frac{\partial}{\partial \boldsymbol{r}}\right). \qquad (\text{II}\cdot3)$$

For the isothermal atmosphere, we may put

$$\frac{\rho(T)}{\rho(t)} = \frac{T}{t}. \qquad (\text{II}\cdot4)$$

Here, as shown in §3, after the Fourier transformation it is now useful to introduce the following new variables, ζ and t, instead of using the Eyges transformations, defined by

$$\left.\begin{aligned}\zeta &= xT(\ln\xi - \ln t'),\\ t &= t'.\end{aligned}\right\} \qquad (\text{II}\cdot5)$$

Then, we get $\dfrac{\partial}{\partial t} - \dfrac{T}{t}\left(x\dfrac{\partial}{\partial \zeta}\right) = \dfrac{\partial}{\partial t'}$. Landau's equation for the isothermal atmosphere is now given by

$$\left[\frac{\partial^2}{\partial t'^2} + (A' + \sigma_0)\frac{\partial}{\partial t'} + (A'\sigma_0 - B'C')\right]f$$

$$= \left(\frac{\partial}{\partial t} + \sigma_0\right)\left[-\frac{E_s^2 x^2}{4E^2}T^2(\ln\xi - \ln t')^2 + \varepsilon\frac{\partial}{\partial E}\right]f. \qquad (\text{II}\cdot6)$$

The solution of this equation is identical with the structure function for the constant air density except the different definition of $\mathfrak{M}$, which is given in this case by

$$L(s+2p+q)M(p,q,s,t) = \left(\frac{\partial}{\partial t'}+\sigma_0\right)\{pT^2(\ln\xi-\ln t')^2M(p-1,q,s,t)$$

$$+ (s+2p+q)qM(p,q-1,s,t)\} \tag{II·7}$$

with

$$\mathfrak{M} = \lim_{\xi-t\to 0} M.$$

In order to get the solution of the diffusion equation, we first develop $(\ln\xi-\ln t')^2$ as

$$(\ln\xi-\ln t')^2 = \frac{(\xi-t')^2}{\xi^2}\left(1+\frac{(\xi-t')}{\xi}+\frac{11}{12}\frac{(\xi-t')^2}{\xi^2}+\frac{5}{6}\frac{(\xi-t')^3}{\xi^3}+\cdots\right).$$
$$\tag{II·8}$$

If we develop $\mathfrak{M}$ as

$$\mathfrak{M} = \lim_{\xi\to T} T^2\left(\frac{\mathfrak{M}_0}{\xi^2}+\frac{\mathfrak{M}_1}{\xi^3}+\cdots\right), \tag{II·9}$$

then $\mathfrak{M}_0$ is just the same function as the one obtained in homogeneous matter.

The consequence corresponds to the fact that the structure function in the isothermal atmosphere is, as a first approximation, given by the structure function in homogeneous matter with the density at the observation point, because the series (II·9) converges very rapidly.

As was shown in §7, $\langle r^2\rangle_{av.}$ is proportional to $\mathfrak{M}(p=1)$, then from the series(II·9) it may be approximated by

$$\langle r^2\rangle_{av.} \sim \frac{T^2\mathfrak{M}_0(p=1)}{\left(T-\frac{\mathfrak{M}_1}{2\mathfrak{M}_0}\right)^2}. \tag{II·10}$$

Then we should measure the length by cascade unit at $\frac{\mathfrak{M}_1}{2\mathfrak{M}_0}$ cascade unit above the observation point for making the comparison between the theoretical curve and the experimental data.

As was shown in the paper of Bhabha-Chakraberty[12], the exact solution of equation (II·7) for $p=n$, $q=0$ is given by

$$\mathfrak{M}(p=n,q=0) = \lim_{(\xi-T)\to 0} n\int_0^T \mathfrak{M}(0,0,s+2n,T-t)T^2(\ln\xi-\ln t)^2$$

$$\times M(p=n-1,q=0,s,t)dt, \tag{II·11}$$

which may be interpreted as the general extention of the Roberg-Nordheim formula, and which also corresponds exactly to the solution given by Messel and Green.

The numerical calculations of $\dfrac{\mathfrak{M}_1}{2\mathfrak{M}_0}$ are carried out both in the approximation A and B for several ages, and the results are shown in Table 8.

Table 8

Numerical Results of $\dfrac{1}{2}\dfrac{\mathfrak{M}_1}{\mathfrak{M}_0}$ in the approximation A.

s	0.6	1.0	1.4	2.0
$\dfrac{1}{2}\dfrac{\mathfrak{M}}{\mathfrak{M}_0}$	0.98	1.75	3.3	7.43

In the approximation B, the value of $\dfrac{\mathfrak{M}_1}{2\mathfrak{M}_0}$ is approximately given by $\dfrac{3}{2\sigma_0}$ which hardly depends on s because $\sigma_0 = 0.7733$.

Thus it seems reasonable for the comparison of theory with experiment to take the air density at about two cascade units above from the observation point.

III. Numerical calculations of the structure function near the core for the finite incident energy

In §3, we have presented the numerical results of the lateral structure function which were calculated assuming that the parent energy of a cascade is infinitely high. In the vicinity of the shower axis, however, the mean energy of shower particles is so high that the parent energy E_0 of the shower can no longer be regarded as infinitely large. Furthermore, as the core structure of the extensive air showers would provide a powerful clue to the knowledge of the angular spread of the source particles, it is desirable to separate the core spread due to the spread of the parent particles emitted in the high energy nuclear interactions from that due to the Coulomb scattering of shower particles in the cascade. Then it seems necessary to present the detailed behavior of the structure function near the shower axis, and to estimate to what degree the structure function of a certain finite incident energy deviates from that of the infinite incident energy.

To get the structure functions for the finite incident energies, we first define the ratio as

$$R(E_0, r, s) = \frac{P_{\mathrm{II}_2}(E_0 \neq \infty, r, s)}{P_{\mathrm{II}_2}(E_0 = \infty, r, s)} .$$

(III·1)

The numerical calculation of $R(E_0)$ is simpler than that of the direct calculation of $P_{\Pi_2}(E_0 \neq \infty, r, s)$ itself.

As the structure function $P_{\Pi_2}(E_0 = \infty)$ for the infinite parent energy was already obtained in §3, $R(E_0)P_{\Pi_2}(E_0 = \infty)$ gives the structure function for a certain finite value of E_0. The numerical calculation of $R(E_0, r, s)$ can be performed approximately in the following way.

At first, from the equation

$$\lambda_1'(s)t + \ln(E_0/\varepsilon) - \frac{1}{2}\psi\left(1 - \frac{s}{2}\right) = 0, \tag{III·2}$$

where $\psi(x) = \dfrac{d}{dx}\ln\Gamma(x)$, we evaluate t for the certain values of (E_0/ε) and s. The age parameter s appearing in (III·2) is the same one defined in the one-dimensional cascade theory, and so represents the age of the shower as a whole at the depth t.

Next, using the value of t thus obtained, the value of s' is evaluated for a certain value of r/r_1 from the equation

$$\lambda_1'(s')t + \ln(E_0/\varepsilon) - \frac{1}{2}\psi\left(1 - \frac{s}{2}\right) + \ln(r/r_1) = 0. \tag{III·3}$$

The value of s' here obtained depends upon the distance from the axis, r/r_1, and $s' = s$ for $r = r_1$. This s' is the one which should be used for the calculation of the structure function for a finite value of E_0/ε. Then the ratio $R(E_0)$ is given by

$$R(E_0) = \frac{\mathfrak{M}_2\left(-\dfrac{s'}{2}\right)}{\mathfrak{M}_2\left(-\dfrac{s}{2}\right)} \frac{\Gamma\left(1 - \dfrac{s'}{1}\right)}{\Gamma\left(1 - \dfrac{s}{2}\right)} \sqrt{\frac{\lambda_1''(s)t + \dfrac{1}{4}\psi'\left(1 - \dfrac{s}{2}\right)}{\lambda_1''(s')t + \dfrac{1}{4}\psi'\left(1 - \dfrac{s'}{2}\right)}}$$

$$\times \exp\left[\Delta s\{\ln(E_0/\varepsilon) + \ln(r/r_1)\} + \{\lambda_1(s') - \lambda_1(s)\}t\right], \tag{III·4}$$

where $\psi'(x) = \dfrac{d^2}{dx^2}\ln\Gamma(x)$, and $\Delta s = s' - s$.

The numerical results of $P_{\Pi_2}(E_0, r, s) = R(E_0)P_{\Pi_2}(E_0 = \infty, r, s)$ are shown in Figs. 16 and 17 for $s = 1.0$ and 1.4 respectively for several different values of E_0/ε.

As can be seen from these figures, the structure functions for the finite incident energies become flatter near the shower axis when compared with the one for an infinite incident energy. The deviation occurs within about one tenth of Moléire unit, and the lower the incident energy and the shorter the distance from the axis, the larger the deviation becomes.
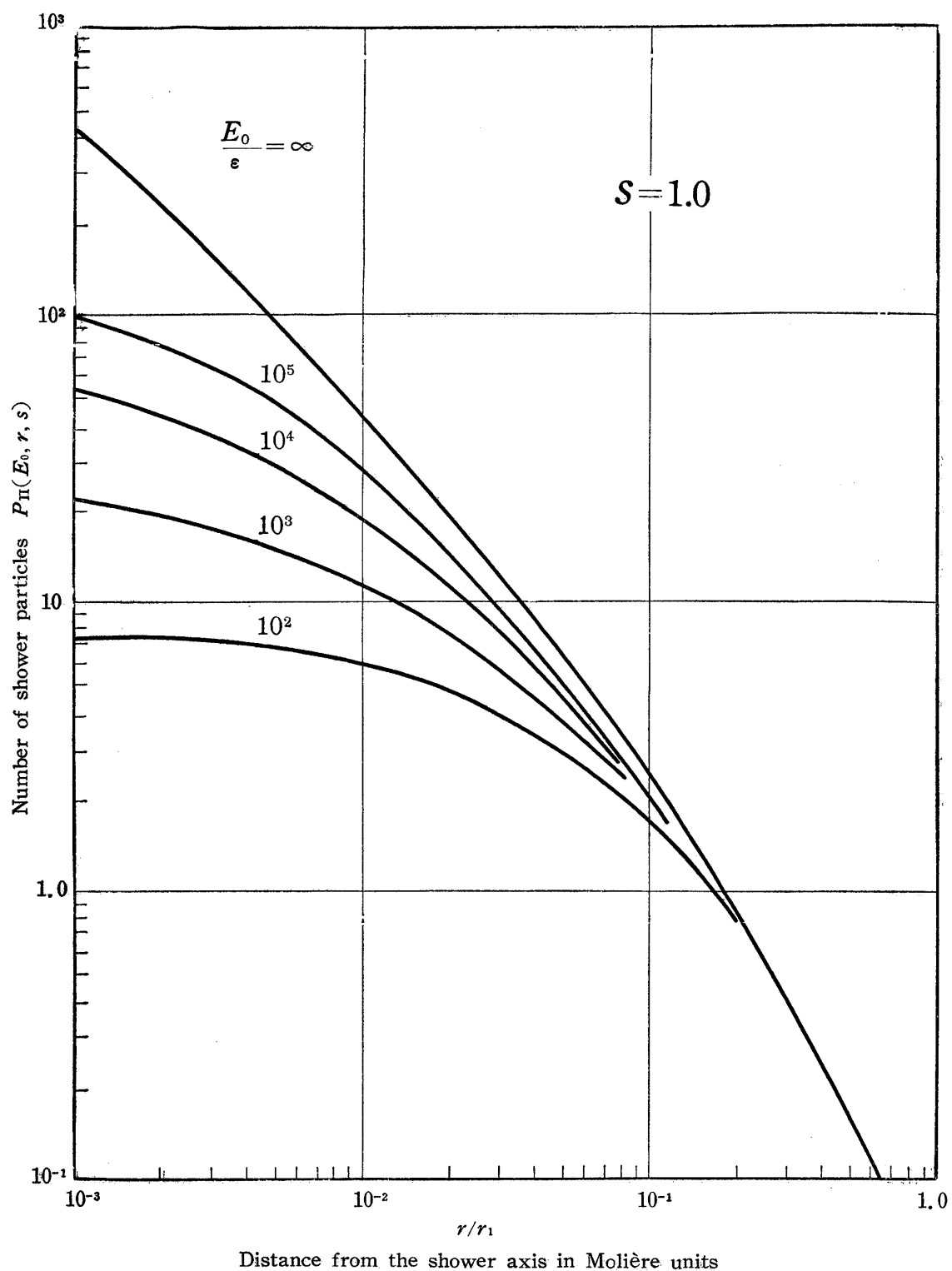
Fig. 16. Structure Function for the finite incident energy. $s=1.0$. The number attached to each curve represents the incident energy of the shower in terms of the critical energy.
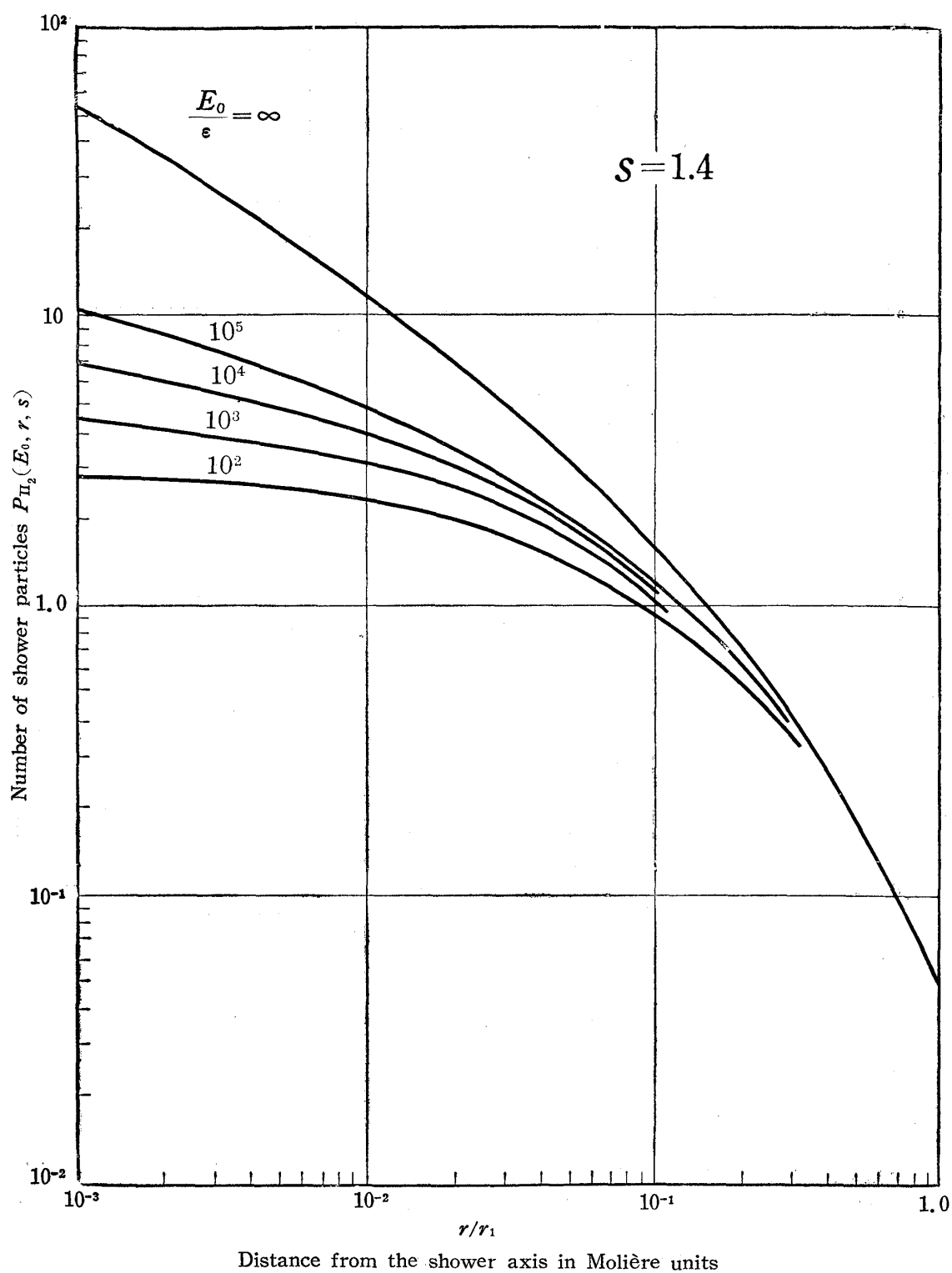
Fig. 17. Structure Function for the finite incident energy. $s=1.4$. The number attached to each curve represents the incident energy of the shower in terms of the critical energy.

IV. Numerical evaluations of $\mathfrak{M}(p, q, s, t)$

For the actual numerical evaluation of the structure functions, it is necessary to get the numerical values of $\mathfrak{M}(p, q, s, t)$ from the difference equation in §3. A similar difference equation already appeared and was treated in the usual linear cascade theory, and in fact, the equation defining $\mathfrak{M}(p=0, q, s, t)$ coincides with the usual difference equation appearing in the linear cascade theory[12),13]. This is because, if we neglect the effect of the Coulomb scattering, the structure function obtained in §3 and §4 must be the linear cascade function, and in this case $\mathfrak{M}(p, q, s, t)$ appears only in the form of $\mathfrak{M}(p=0, q, s, t)$ in the structure function.

As is shown in the paper of Bhabha-Chakrabarty[13], the solution of the difference equation (3·38) is given by

$$M(p, q, s, t, \xi-t) = \int_0^t \mathfrak{M}(0, 0, s+2p+q, t-t')$$

$$\times \{p(\xi-t)^2 M(p-1, q, s, t', \xi-t')$$

$$+q(s+2p+q) M(p, q-1, s, t', \xi-t')\} dt'. \tag{IV·1}$$

Under a certain boundary condition, we can obtain the numerical values of $\mathfrak{M}(p, q, s, t)$ for any values of positive integer p and q using the above formula.

As is easily seen from the above solution, $\mathfrak{M}(p, q, s, t)$ is usualy represented by a polynomial containing $e^{\lambda_1(s)t}$, $e^{\lambda_1(s+1)t}$, $\cdots\cdots\cdots$, $e^{\lambda_2(s)t}$, $e^{\lambda_2(s+1)t}$, $\cdots\cdots\cdots$, in which all the terms except those containing $e^{\lambda_1(s)t}$ can be neglected provided $t \gg 1$.

Another different approach for obtaining the numerical values of $\mathfrak{M}_1(p, q, s, t)$ is the operational calculation.

The equation (3·38) can now be written in an operational form as

$$M(p, q, s, t, \xi-t) = \frac{\dfrac{\partial}{\partial t}+\sigma_0}{\left(\dfrac{\partial}{\partial t}-\lambda_1(s+2p+q)\right)\left(\dfrac{\partial}{\partial t}-\lambda_2(s+2p+q)\right)}$$

$$\times [p(\xi-t)^2 M(p-1, q, s, t, \xi-t)$$

$$+q(s+2p+q) M(p, q-1, s, t, \xi-t)]. \tag{IV·2}$$

Putting $q=0$, we get

$$M(p, 0, s, t, \xi-t) = \left(\frac{H_1(s+2p)}{\dfrac{\partial}{\partial t}-\lambda_1(s+2p)} + \frac{H_2(s+2p)}{\dfrac{\partial}{\partial t}-\lambda_2(s+2p)}\right)$$

$$\times \{p(\xi-t)^2 M(p-1, 0, s, t, \xi-t)\}. \tag{IV·3}$$

Then if we limit ourselves to the terms containing $e^{\lambda_1(s)t}$, it can be written as

$$M(p,0,s,t,\xi-t)=e^{\lambda_1(s)t}\left[\frac{H_1(s+2p)}{\frac{\partial}{\partial t}+\lambda_1(s)-\lambda_1(s+2p)}\right.$$

$$\left.+\frac{H_2(s+2p)}{\frac{\partial}{\partial t}+\lambda_1(s)-\lambda_2(s+2p)}\right][p(\xi-t)^2M(p-1,0,s,t,\xi-t)e^{-\lambda_1(s)t}].$$

$$\text{(IV·4)}$$

The above expression gives approximate values of $\mathfrak{M}_2(p,q,s,t)$ with positive integer p for $t\gg1$.

For the values of $\mathfrak{M}_1(p,q,s,t)$ appearing in the angular structure function, we can put $\xi-t=1$. If we limit ourselves to the terms containing $e^{\lambda_1(s)t}$, we get

$$\mathfrak{M}_1(p,0,s,t)=p\mathfrak{M}_1(p-1,0,s,t)\left[\frac{H_1(s+2p)}{\lambda_1(s)-\lambda_1(s+2p)}+\frac{H_2(s+2p)}{\lambda_1(s)-\lambda_2(s+2p)}\right]$$

$$=L(p)\mathfrak{M}_1(p-1,0,s,t).$$

$$\text{(IV·5)}$$

Since $\lim\limits_{l\to\infty}\dfrac{L(l+1)}{L(l)}=1$, $\mathfrak{M}_1(p,0,s,t)$ for any value of p is given by

$$\mathfrak{M}_1(p,0,s,t)=\lim_{l\to\infty}\frac{L(l)^{1+\delta}L(l-1)\cdots\cdots L(1)}{L(l+\delta)\cdots\cdots L(n+\delta+1)},$$

$$\text{(IV·6)}$$

where $n+\delta=p$ and n is the integer.

For the values of $\mathfrak{M}_2(p,0,s,t)$ any simple approximate formula similar to that of $\mathfrak{M}_1$ cannot be obtained, because in this case $\dfrac{\partial}{\partial t}$ operates $(\xi-t)^2$ in the formula (IV·3). The value of $\mathfrak{M}_2(p,0,s,t)$ for any value of p is obtained by an interpolation using the values of $\mathfrak{M}_1(p,0,s,t)$ for the positive integer p.

For the negative values of p, $\mathfrak{M}(p,0,s,t)$ has a pole at $p=-\dfrac{s}{2}-\dfrac{1}{3}$. Thus π_2 is represented by $1/r^{2-s-(2/3)}$ near the shower axis as shown in the formula (3·43).

The existence of the pole at $p=-\dfrac{s}{2}-\dfrac{1}{3}$ can be proved as follows: Let

$$G(x)=\sum_{p=0}^{\infty}\frac{(-x^2)^p}{\Gamma(p+1)}M(p,0,s,t)=\frac{1}{2\pi i}\int_{-i\infty}^{+i\infty}\Gamma(-p)x^{2p}M(p,0,s,t)dp$$

$$\text{(IV·7)}$$

be the generating function of $\mathfrak{M}_2(p,0,s,t)$, then $G(x)$ satisfies the following equation:

$$\left[\frac{\partial}{\partial t'}+A'-\frac{B'C'}{\dfrac{\partial}{\partial t}+\sigma_0}\right]G=-x^2(\xi-t)^2G. \tag{IV·8}$$

The solution of this equation is

$$G=e^{\frac{x^2(\xi-t)^3}{3}}\int_{\xi-t}^{\infty}e^{\frac{-x^2(\xi-t')^3}{3}}\left[A'-\frac{B'C'}{\dfrac{\partial}{\partial t}+\sigma_0}\right]Gdt',$$

where the upper and the lower limits of the integral are determined using the property that G must be zero at the limit $\xi-t=\dfrac{\zeta}{x}=\infty$.

Now the first term in the above integrand implies a factor

$$A'G=\int_0^1[G(x)-(1-v)^sG(x(1-v))]\varphi(v)dv. \tag{IV·9}$$

This is reduced to

$$A'G=\int_0^1[G(x)-v^sG(xv)]\varphi(v)dv$$

$$=\int_0^x\left[G(x)-\left(\frac{y}{x}\right)^sG(y)\right]\varphi\left(1-\frac{y}{x}\right)\frac{dy}{x}.$$

At the limit $x=\infty$

$$A'G=\int_0^\infty\left[G(x)-\left(\frac{y}{x}\right)^sG(y)\right]\varphi\left(1-\frac{y}{x}\right)\frac{dy}{x},$$

and remembering

$$\varphi\left(1-\frac{y}{x}\right)\approx\frac{1}{1-(y/x)}=1+\frac{y}{x}+\cdots\cdots,$$

we get

$$\lim_{x\to\infty}A'G=\lim_{x\to\infty}G(x)=\lim_{x\to\infty}\frac{1}{x^{s+1}}\sum_n a_n(\xi-t)^n. \tag{IV·10}$$

In the second term in the integrand there appears

$$B'C'G(x(\xi-t),x)=2\int_0^1\psi(u)\,du\int_0^u G(xv(\xi-t),xv)v^s\varphi\left(\frac{v}{u}\right)\frac{dv}{u}$$

$$=2\int_0^1\psi(u)\,du\int_0^{xu}G(y(\xi-t),y)y^sx^s\varphi\left(\frac{y}{ux}\right)\frac{dy}{ux}.$$

At the limit $x=\infty$, the above formula becomes

$$B'C'G = 1.36 \frac{B(0)}{x^s} \int_0^\infty G(y(\xi-t), y) y^{s-1} dy. \tag{IV·11}$$

Putting

$$\int_0^\infty G y^{s-1} dy = \sum b_n (\xi-t)^n,$$

we get

$$\lim_{x \to \infty} \frac{B'C'G}{\frac{\partial}{\partial t} + \sigma_0} = \frac{1.36 B(0) e^{\sigma_0 (\xi-t)}}{x^s} \int_{(\xi-t)}^\infty e^{-\sigma_0 (\xi-t')} dt' \int_0^\infty G y^{s-1} dy. \tag{IV·12}$$

To see the behavior of G at $x = \infty$, we take the lowest order of power of $1/x$ in the above expressions (IV·10) and (IV·12).

Thus the solution of (IV·8) becomes at the limit of $x = \infty$

$$\lim_{x \to \infty} G = e^{\frac{x^2 (\xi-t)^3}{3}} \int_{(\xi-t)}^\infty e^{-\frac{x^2 (\xi-t')^3}{3}} \sum_n \frac{c_n}{x^s} (\xi-t')^n dt'. \tag{IV·13}$$

Putting $(\xi-t')^3 = z$, we get

$$\lim_{(\xi-t) \to 0} G = \lim_{(\xi-t) \to 0} e^{\frac{x^2 (\xi-t)^3}{3}} \int_{(\xi-t)}^\infty \frac{e^{-\frac{x^2 z}{3}}}{3 x^3} z^{-2/3} \sum c_n z^{n/3} dz$$

$$= \sum \frac{1}{3} c_n \Gamma\left(\frac{1}{3}\right) \left(\frac{x^2}{3}\right)^{-(1/3)-(n/3)} x^{-s}. \tag{IV·14}$$

Remembering the definition (IV·7), we can conclude that $\mathfrak{M}_2(p, 0, s, t)$ has a simple pole at $p = -(s/2) - (1/3)$. After finding this pole, an extrapolation is made for the values of $\mathfrak{M}_2(p, 0, s, t)$ from the positive side to the negative side of the p-plane.

A similar argument is also made for $\mathfrak{M}_1(p, 0, s, t)$ in the angular distribution function, and it can be shown that $\mathfrak{M}_1$ has a simple pole at $p = -(s/2) - 1$ instead of $-(s/2) - (1/3)$.

After obtaining the values of $\mathfrak{M}(p, 0, s, t)$, we can solve the equation by varying q for fixed values of p.

Then, we get $\mathfrak{M}(p, q, s, t)$ with any values of p and q.

References

1) L. Eyges and S. Fernbach, Phys. Rev. **82** (1951), 23.

2) B. A. Chartres and H. Messel, Phys. Rev. **104** (1956), 517.

3) G. Molière, Cosmic Radiation, edited by W. Heisenberg, (1946).

4) B. Rossi and K. Greisen, Rev. Mod. Phys. **13** (1941), 240.

5) J. Roberg and L. W. Nordheim, Phys. Rev. **75** (1949), 444.

6) J. Nishimura and K. Kamata, Prog. Theor. Phys. **6** (1951), 262, 628.
   7 (1952), 185.

7) I. B. Bernstein, Phys. Rev. **80** (1950), 995.

8) L. Landau and I. Pomeranchuk, Dokl. Akad. Nauk. **92** (1956), 535.

9) E. J. Williams, Proc. Roy Soc. **169** (1939), 531.

10) R. Hofstadter, Rev. Mod. Phys. **28** (1956), 214.

11) L. Landau and G. Rumer, Proc. Roy, Soc. **166** (1938), 531.

12) H. J. Bhabha and S. K. Chakrabarty, Phys. Rev. **74** (1948), 1352.

13) H. S. Snyder, Phys. Rev. **76** (1949), 1563.

14) I. Pomeranchuk, J. Phys. U. S. S. R. **8** (1944) 17.

15) H. S. Snyder and W. T. Scott, Phys. Rev. **76** (1952), 220.
    G. Molière, Z. Naturforsh. **3a** (1948), 1801.

16) L. Eyges, Phys. Rev. **74** (1948), 1801.

17) N. A. Porter, Oxford Conf. (1956).
    T. Matano, I. Miura, M. Oda, K. Suga, G. Tanahashi and Y. Tanaka. Varenna Conf. (1957).

18) K. Pinkau, Phil. Mag. **2** (1957), 1389.

19) Cooperative Emulsion Group in Japan, will be published soon in Nuovo Cimento.

20) S. P. Dobrovol' skii, S. I. Nikol'skii, E. I. Tukisii and V. I. Iakovlev, J. Expl. Theo. Phys. U. S. S. R. **31** (1956), 939.

21) H. S. Green and H. Messel, Phys. Rev. **88** (1952), 331.

22) H. S. Green and O. Bergmann, Phys. Rev. **95** (1954), 516.

23) K. Greisen, Prog. Cosmic-ray Physics, Vol. III, edited by J. G. Wilson (1956).